Towards Interpretability Without Sacrifice: Faithful Dense Layer Decomposition with Mixture of Decoders

James Oldfield[m,q*] **Shawn Im**[m] **Yixuan Li**[m] **Mihalis A. Nicolaou**[c]
Ioannis Patras[q] **Grigorios G Chrysos**[m]

[m] University of Wisconsin–Madison [q] Queen Mary University of London [c] The Cyprus Institute

Abstract

Multilayer perceptrons (MLPs) are an integral part of large language models, yet their dense representations render them difficult to understand, edit, and steer. Recent methods learn interpretable approximations via neuron-level sparsity, yet fail to faithfully reconstruct the original mapping–significantly increasing model's next-token cross-entropy loss. In this paper, we advocate for moving to *layer*-level sparsity to overcome the accuracy trade-off in sparse layer approximation. Under this paradigm, we introduce Mixture of Decoders (MxDs). MxDs generalize MLPs and Gated Linear Units, expanding pre-trained dense layers into tens of thousands of specialized sublayers. Through a flexible form of tensor factorization, each sparsely activating MxD sublayer implements a linear transformation with full-rank weights–preserving the original decoders' expressive capacity even under heavy sparsity. Experimentally, we show that MxDs significantly outperform state-of-the-art methods (e.g., Transcoders) on the sparsity-accuracy frontier in language models with up to 3B parameters. Further evaluations on sparse probing and feature steering demonstrate that MxDs learn similarly specialized features of natural language–opening up a promising new avenue for designing interpretable yet faithful decompositions. Our code is included at: https://github.com/james-oldfield/MxD/.

1 Introduction

One strategy for addressing concerns about large language models' (LLMs) [1, 2, 3] behavior is via a bottom-up approach to understanding and controlling the network internals–developing models of how and where human-interpretable features are represented in LLMs and how they affect the output [4, 5, 6]. Such a mechanistic understanding has proved helpful for a number of issues relating to safety and transparency, from controlling refusal of harmful requests [7] to detecting generation of unsafe code [6] and latent model knowledge [8].

However, developing models of LLMs' internals faces challenges due to the dense nature of their representations [9, 10]. Indeed, many studies have found that individual neurons in MLP layers encode *multiple* distinct concepts. Rather than human-interpretable features being neatly aligned with individual neurons, they are often distributed across many [11, 12]. As a result, it is not straightforward to cleanly isolate specific concepts of interest in the models' latent token representations.

Traditionally, imposing constraints on model form has offered a way to instill more predictable properties or structure. Indeed, there is a rich history of success with constraints in machine learning: from parts-based representations through non-negativity [13, 14], to structure through low-rankness or assumptions on geometry [15, 16]. With the particular issues posed by dense representations in LLMs, *specialization through sparsity* has re-emerged as a dominating strategy for learning

*Corresponding author: j.a.oldfield@qmul.ac.uk. Work done whilst at UW-Madison.

Preprint. Under review.

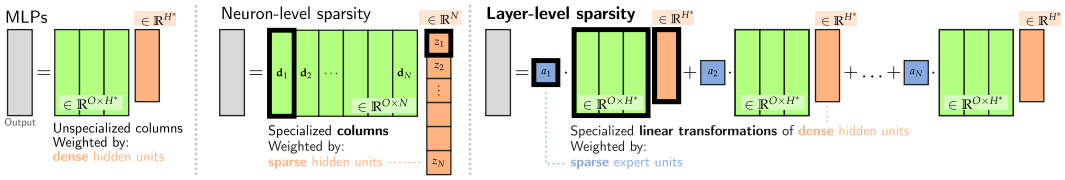

Figure 1: **Units of specialization for sparse layer variants**: *Neuron*-level sparsity of existing sparse MLPs [27, 26] (center) vs *layer*-level sparsity (right), which the proposed Mixture of Decoders (MxD) layer enables at scale. For `GPT2-124M`, the dimensions are: $O = 768$, $H^* = O \cdot 4$, $N \approx O \cdot 32$.

more interpretable representations. With prior work showing that sparser models both aid human explanation [17] and achieve higher scores on LLM-based auto-interpretability metrics [18, 19], sparsity is often used as a proxy for interpretability [20, 21]. To this end, many recent works–such as sparse autoencoders [22, 23, 6]–take inspiration from traditional sparse dictionary learning methodologies [24, 25], re-writing pre-trained LLMs' activations as sparse, non-negative linear combinations of atoms in a learned overcomplete basis. However, as argued in [26], such approaches do not learn the functional mechanisms of LLMs' layers, and their inherent post-hoc nature demands additional parameters and computation on top of the base models.

One alternative approach is to directly replace layers with more interpretable equivalents [28], such as with wide MLPs with sparsity constraints. Transcoders [27, 29, 30, 26] (TCs) are a recent example of this, training new MLPs to mimic the functional behavior of MLPs with *sparse* hidden units, which have recently been shown to also learn more interpretable features [26]. Thus, instead of relying on external post-hoc analysis, sparse MLP layers offer a way to distill specialized features directly into the model's forward pass itself.

Both of the above methods for learning specialized features fall into the same category of what one may call 'neuron-level sparsity'. Dictionary learning methods restrict the number of non-zero elements used from a learned dictionary, whilst sparse MLPs [27] limit the number of active rows used from a learned 'decoder' matrix. At its core, whilst this constraint is useful for interpretability, it is too restrictive–often heavily trading off accuracy for sparsity, poorly reconstructing the original model components [31, 28]. We argue that preserving the base models' performance is a crucial component of sparse MLP layer approximations for the following two key reasons:

1. **Model faithfulness**: sparse layers that poorly approximate the original layers risk missing critical intricacies of the base models' behavior or latent features [32]. Conversely, an accurate reconstruction (yielding similar downstream next-token loss) is some evidence that the combination of newly learned subcomputations faithfully emulates the base model.
2. **Practical adoption**: sparse layers that closely preserve base models' performance are capable of *replacing* the existing MLPs, directly integrating specialized computation into the native forward pass. Otherwise, downstream use of the sparse layers' features must run on top of the base models' computation. This introduces additional inference-time cost to every forward pass, and restricts any analysis to post-hoc settings.

In this paper, we advocate for moving from *neuron*-level to *layer*-level sparsity (as illustrated in Figure 1) to address this. We propose the *Mixture of Decoders (MxD)* layer to overcome the sparsity-accuracy trade-off through scalable, resource-efficient conditional computation. Rather than individual vectors, MxDs learn interpretable sublayers as atomic units of specialization. This faithfully mirrors the functional form of dense layer we wish to approximate, and allows MxDs to readily generalize to modern MLP variants (i.e., the Gated Linear Unit [33]).

At a technical level, MxDs are constructed via a flexible tensor factorization [34] with the Hadamard product [35]. Through their parameter efficiency, MxDs scale the number of specialized layers far beyond what is feasible with classic sparse mixture of experts (MoEs) [36], and recover prior adapter-based MoEs [37, 38] as a special case. Crucially, we prove that the proposed tensor factorization in MxDs leads to each 'expert' sublayer implementing a linear transformation with full-rank weights–allowing faithful reconstruction even under heavy sparsity. Empirically, we demonstrate that MxDs significantly outperform alternative sparse MLP layers such as Transcoders [27] and Skip Transcoders [26] on the sparsity-accuracy frontier. In addition to their faithfulness, MxDs remain competitive with the SOTA on interpretability metrics. **Our contributions can be summarized as follows:**

- We propose *Mixture of Decoders*, an instance of a flexible class of parameter-efficient MoE through Hadamard product-factorized weight tensors.
- We prove that each specialized MxD expert's weights inherit up to the same rank as the original MLP's decoder, providing faithful approximation even in very sparse models.
- Across 108 sparse layers in 4 LLMs (with up to 3B parameters) MxDs (i) pareto-dominate existing techniques on the sparsity-accuracy frontier yet (ii) remain competitive on 34 sparse probing and steering tasks, validating the interpretability of the learned experts.

2 Methodology

We first recall the technical details of language models' MLP layers and existing approaches to sparse approximations in Section 2.1. We then introduce the proposed MxD in Section 2.2, outlining the attractive rank properties it inherits in Section 2.3 and factorized implementation in Section 2.4. We conclude with extensions to modern MLP layers in Section 2.5.

2.1 Preliminaries

Let $\mathbf{x} \in \mathbb{R}^I$ be the pre-MLP latent representation of a specific token at a given layer. Omitting bias terms throughout for brevity, the GPT2-style MLP layer produces the output vector $\mathbf{y} \in \mathbb{R}^O$ as:

$$\text{MLP}(\mathbf{x}) = \mathbf{D}^{*\top}\mathbf{z}^* \in \mathbb{R}^O, \quad \text{with } \mathbf{z}^* := \phi\big(\mathbf{E}^{*\top}\mathbf{x}\big) \in \mathbb{R}^{H^*}, \tag{1}$$

where $\mathbf{E}^* \in \mathbb{R}^{I\times H^*}$, $\mathbf{D}^* \in \mathbb{R}^{H^*\times O}$ are the learnable 'encoder' and 'decoder' parameters respectively, and $\phi(.)$ is an activation function, often a GELU [39]. We use * to denote the weights/dimensions of the pre-trained base LLM.

Sparse approximations One approach to learning interpretable features in MLPs is to train new, wider MLPs with *sparse* hidden units to reconstruct the original layer's outputs [27, 26, 30, 29], reminiscent of dictionary learning techniques [25]. In general, sparse MLPs share the model form:

$$\text{SMLP}(\mathbf{x}) = \mathbf{D}^\top\mathbf{z} = \sum_{h=1}^{H} z_h\mathbf{d}_h \in \mathbb{R}^O, \quad \text{with } \mathbf{z} := \mathcal{S}\big(\mathbf{E}^\top\mathbf{x}\big) \in \mathbb{R}^H, \tag{2}$$

where $\mathcal{S}(.)$ is a sparsity-inducing function (such as the top-K [23] activation used in this paper). Here, the dimensionality of sparse MLPs' learnable weights $\mathbf{E} \in \mathbb{R}^{I\times H}$, $\mathbf{D} \in \mathbb{R}^{H\times O}$ are set as $H \gg H^*$ such that the hidden layer is significantly larger than that of the original MLP. The original post-MLP output vectors are approximated as a K-sparse, non-negative linear combination of the rows $\mathbf{d}_n$ of a newly learned decoder matrix. Whilst this model form has been shown to learn interpretable, specialized features z_h in language models [27, 26], their poor reconstruction is of questionable faithfulness and limits their use as a layer replacement in practice.

2.2 Mixture of Decoders

We now detail the proposed Mixture of Decoders (MxD) layer, which overcomes the sparsity-accuracy trade-off by treating sparsely activating linear layers as the atomic unit of specialization. We approximate the original MLP with a conditional combination of N *linear transformations*:

$$\text{MxD}(\mathbf{x}) = \sum_{n=1}^{N} a_n(\mathbf{W}_n^\top\mathbf{z}) \in \mathbb{R}^O, \tag{3}$$

where $\mathbf{a} := \mathcal{S}\big(\mathbf{G}^\top\mathbf{x}\big) \in \mathbb{R}^N$ are *sparse* 'expert coefficients' from learnable gating matrix $\mathbf{G} \in \mathbb{R}^{I\times N}$, and $\mathbf{z} := \phi\big(\mathbf{E}^\top\mathbf{x}\big) \in \mathbb{R}^H$ is the *dense* output from an encoder. Here, $\boldsymbol{\mathcal{W}} \in \mathbb{R}^{N\times H\times O}$ is a third-order tensor of parameters collating all N experts' decoder weights $\boldsymbol{\mathcal{W}}(n,:,:) = \mathbf{W}_n \in \mathbb{R}^{H\times O}$. In MxDs, we use a large N to scale the feature specialization, and set $H := H^*$ to match the original MLP's smaller hidden dimension.

With the gate routing each token to just its top-K experts, each $\mathbf{W}_n \in \mathbb{R}^{H\times O}$ receives a gradient signal from only a specific set of semantically similar tokens. This implicit clustering naturally leads

experts to specialize in feature-specific subcomputations, while collectively covering the layer's full functionality. MxDs in Equation (3) also directly inherit the MLP layers' original functional form, avoiding the need to impose sparsity and non-negativity constraints on the hidden units $\mathbf{z} \in \mathbb{R}^H$. However, MxD decoders naively require a prohibitive NHO parameters–preventing N from scaling to tens of thousands of specialized components. To achieve parameter-efficiency whilst retaining layer capacity for faithful layer approximation, we parameterize MxDs' third-order weight tensor $\boldsymbol{\mathcal{W}} \in \mathbb{R}^{N\times H\times O}$ specifically to yield full-rank expert weights, defined elementwise as:

$$\boldsymbol{\mathcal{W}}(n,h,:) = \mathbf{c}_n * \mathbf{d}_h \in \mathbb{R}^O, \qquad \forall\, n \in \{1,\dots,N\},\ h \in \{1,\dots,H\}, \tag{4}$$

where $*$ is the *Hadamard product* [34, 35], and $\mathbf{c}_n,\ \mathbf{d}_h \in \mathbb{R}^O$ are the rows of learnable weights $\mathbf{C} \in \mathbb{R}^{N\times O}$, $\mathbf{D} \in \mathbb{R}^{H\times O}$. Intuitively, $\mathbf{D}$ implements a base transformation modulated by the N specialized units in $\mathbf{C}$. Additional technical motivation for this parameterization with tensor methods can be found in Appendix A.3. This brings MxDs' parameter count down significantly to $O\cdot(N+H)$ from NHO in Equation (3) with N full decoders. One can then vary N to parameter-match sparse MLP layers. We next detail how this design (i) retains expressivity in each unit for faithful layer approximation under sparsity in Section 2.3 and (ii) yields a simple forward pass in Section 2.4.

2.3 MxDs are rank-preserving

In the original LLM, the linear transformation from the hidden units to the output is constrained by the rank of the original MLP's decoder matrix $\mathbf{D}^* \in \mathbb{R}^{H^*\times O}$. Under only mild technical conditions, *every* expert's weight matrix in MxDs inherits the rank of $\mathbf{D} \in \mathbb{R}^{H\times O}$, thus allowing it to match that of the original MLP's decoder, despite its parameter-efficiency:

Lemma 1 (Decoder rank preservation)**.** *We can materialize linear expert n's weight matrix as $\boldsymbol{\mathcal{W}}(n,:,:) = \mathbf{W}_n = \mathbf{D}\,\mathrm{diag}\,(\mathbf{c}_n) \in \mathbb{R}^{H\times O}$. Assuming $\mathrm{diag}\,(\mathbf{c}_n) \in \mathbb{R}^{O\times O}$ is a diagonal matrix with no zeros along its diagonal (and thus invertible), we then have*

$$\mathrm{rank}(\mathbf{W}_n) = \mathrm{rank}(\mathbf{D}\,\mathrm{diag}(\mathbf{c}_n)) = \mathrm{rank}(\mathbf{D}).$$

The proof is found in Appendix A.1, which first derives the matrix-valued expression for each expert from Equation (4) and then applies a standard rank equality. At a sparsity level of K, each MxD output vector is a weighted sum of K-many linear transformations (each with potentially full-rank weights) of the dense hidden units $\mathbf{z}$. As a result, MxDs retain layer capacity even under high sparsity. Sparse MLPs' hidden units have only K non-zero elements in contrast–each output in Equation (2) is therefore confined to a K-dimensional subspace of $\mathbb{R}^O$, potentially limiting the capacity of sparse MLPs to faithfully approximate the original mapping in the small K regime desirable for interpretability (mirroring speculations by [26]). Further, whilst alternative soft linear MoEs achieve scalability through low-rankness [40], Lemma 1 states that no such rank constraints are present in MxDs. For approximating existing MLP layers where low-rank assumptions may not hold, MxDs are consequently a more suitable class of conditional layer.

2.4 Factorized forward pass

MxDs compute a linear combination of N linear transformations of the dense vector. With the proposed Hadamard-factorized weights, this yields a simple implementation.

Lemma 2 (Hadamard-factorized MoE forward pass)**.** *Let $\mathbf{z} \in \mathbb{R}^H$ and $\mathbf{a} \in \mathbb{R}^N$ denote the MLP hidden units and expert coefficients respectively. Further, denote the decoder matrices as $\mathbf{C} \in \mathbb{R}^{N\times O}$, $\mathbf{D} \in \mathbb{R}^{H\times O}$ parameterizing $\boldsymbol{\mathcal{W}} \in \mathbb{R}^{N\times H\times O}$. MxD's forward pass can be re-written as:*

$$\mathrm{MxD}(\mathbf{x}) = \sum_{n=1}^{N} a_n\big(\mathbf{W}_n^\top \mathbf{z}\big) = \big(\mathbf{C}^\top \mathbf{a}\big) * \big(\mathbf{D}^\top \mathbf{z}\big). \tag{5}$$

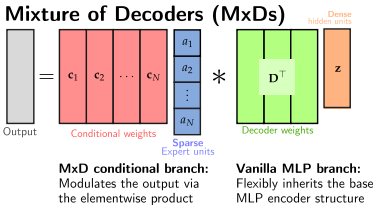

Figure 2: **Mixture of Decoders** extends the base MLP/GLU layers with a conditional 'expert' branch, modulating the MLP's outputs.

The proof is found in Appendix A.2. We include a notebook at https://github.com/james-oldfield/MxD/blob/main/form-equivalence.ipynb showing the equivalence in PyTorch. Further, please see Appendix A.5 for a discussion of how the Hadamard factorization relates to prior parameter-efficient MoEs with element-wise scaling [37].

Table 1: **Model formulations of related work**: $\mathbf{x} \in \mathbb{R}^I$, $\mathbf{y} \in \mathbb{R}^O$ are the pre- and post-MLP representations respectively, $\mathbf{z}$ are the hidden units, and $\mathbf{a}$ is the vector of the 'expert coefficients' for MxD. Model-specific encoders/decoders $\mathbf{E}$, $\mathbf{D}$ map between the hidden units and output.

	MLPs [3]	SAEs [22]	Transcoders [27]	Skip Transcoders [26]	**MxDs (Ours)**
Model form	$\mathbf{y} = \mathbf{D}^{*\top}\mathbf{z}^*$	$\mathbf{y} \approx \mathbf{D}^\top \mathbf{z}$	$\mathbf{y} \approx \mathbf{D}^\top \mathbf{z}$	$\mathbf{y} \approx \mathbf{D}^\top \mathbf{z} + \mathbf{S}^\top \mathbf{x}$	$\mathbf{y} \approx \sum_n a_n \left(\mathbf{W}_n^\top \mathbf{z}\right)$
Sparse component	None	$\mathbf{z} = \mathcal{S}\left(\mathbf{E}^\top \mathbf{y}\right) \in \mathbb{R}^H$	$\mathbf{z} = \mathcal{S}\left(\mathbf{E}^\top \mathbf{x}\right) \in \mathbb{R}^H$	$\mathbf{z} = \mathcal{S}\left(\mathbf{E}^\top \mathbf{x}\right) \in \mathbb{R}^H$	$\mathbf{a} = \mathcal{S}\left(\mathbf{G}^\top \mathbf{x}\right) \in \mathbb{R}^N$

2.5 Extending MxDs to GLUs

In contrast to methods imposing neuron-level sparsity [22, 27, 26], MxDs do not make assumptions about the base layer's encoder architecture or activation function. As a result, MxDs readily generalize to alternative architectures such as the Gated Linear Units (GLUs) [33] used in recent LLMs [1, 2]. Recall that GLUs' hidden units are computed as $\mathbf{z}_{\text{GLU}} = \psi(\mathbf{E}_{\text{GLU}}^\top \mathbf{x}) * \left(\mathbf{E}^\top \mathbf{x}\right) \in \mathbb{R}^H$, with additional GLU parameters $\mathbf{E}_{\text{GLU}} \in \mathbb{R}^{I \times H}$ and GLU activation function ψ (e.g., `Swish` [1]). By substituting in the GLU hidden representations, MxDs straightforwardly extend the GLU model form too:

$$\text{MxD}_{\text{GLU}}(\mathbf{x}) = \sum_{n=1}^{N} a_n \, \mathbf{W}_n^\top \Bigg(\underbrace{\psi(\mathbf{E}_{\text{GLU}}^\top \mathbf{x}) * \left(\mathbf{E}^\top \mathbf{x}\right)}_{\text{GLU hidden units}} \Bigg) = \left(\mathbf{C}^\top \mathbf{a}\right) \; * \; \mathbf{D}^\top \left(\psi(\mathbf{E}_{\text{GLU}}^\top \mathbf{x}) * \left(\mathbf{E}^\top \mathbf{x}\right)\right)$$

where $\mathbf{a} \coloneqq \mathcal{S}\left(\mathbf{G}^\top \mathbf{x}\right) \in \mathbb{R}^N$ are the expert units, and $\mathbf{W}_n = \mathbf{D}\,\text{diag}(\mathbf{c}_n) \in \mathbb{R}^{H \times O}$ as before. For a technical discussion of GLUs and their relationship to MxDs, we refer readers to Appendix A.4– through the theoretical results developed in this paper, we show that GLU encoders themselves can be viewed as a mixture of rank-1 linear experts (in contrast to the rank-preserving MxDs).

3 Experiments

The experimental section in the main paper is split into two parts. Section 3.1 first demonstrates how MxDs perform significantly better on the accuracy-sparsity frontier as sparse MLP layer approximations on 4 LLMs. We then demonstrate in Section 3.2 that MxD's features retain the same levels of specialization through sparse probing and steering evaluations. Thorough ablation studies, experiments with matrix rank, and comparisons to low rank MoEs are presented in Appendix B.

3.1 Sparse approximations of MLPs in LLMs

In this section, we perform experiments approximating LLMs' existing feed-forward layers with sparse MLPs, establishing that MxDs better navigate the sparsity-accuracy frontier, more faithfully approximating the base models' MLPs than the SOTA baseline methods.

Implementation details We train on 4 base models: `GPT2-124M` [3], `Pythia-410m`, `Pythia-1.4b` [41], and `Llama-3.2-3B` [1] with up to 80k experts/features. We train all sparse layers on a total of 480M tokens of OpenWebText [42], with learning rate $1e-4$ and a context length of 128, initializing the output bias as the empirical mean of the training tokens, and $\mathbf{D}$ in MxDs as the zero-matrix (following [26]). We vary N in MxD layers to parameter-match Transcoders in all experiments, with parameter counts and dimensions shown in Table 2. For `Llama3.2-3B`, we use the `Swish-GLU` variant of MxD and `GELU-MLP` MxDs for the other three models, matching the architectures of their base encoders. Through ablation studies in Appendix B.6 we show that MxDs using the GELU/GLU variants are much more accurate layer approximators than the ReLU variants. Full experimental details are included in Appendix D. Whilst we do not have the computational resources to show similarly thorough experiments on even larger LLMs, we expect MxDs to scale just as well to models with tens of billions of parameters or more.

Objective function Given the frozen weights of the MLP, we train sparse layers to minimize the normalized reconstruction loss between its output and that of the original MLP layer with objectives of the form $\mathcal{L} = \mathbb{E}_{\mathbf{x}} \left[\frac{||\text{MLP}(\mathbf{x}) - f(\mathbf{x})||_2^2}{||\text{MLP}(\mathbf{x})||_2} \right]$, where $f(.)$ denotes the various learnable sparse MLP layers.

Table 2: Sparse layer parameters/dimensions: H denotes the size of the layers' hidden units and N is the expert count. MxDs perform almost as many linear transformations as the baselines have features.

	GPT2-124M			Pythia-410M			Pythia-1.4B			Llama-3.2-3B		
Model	Params	H	N	Params	H	N	Params	H	N	Params	H	N
Transcoders [27]	37.7M	24,576	—	67.1M	32,768	—	268.5M	65,536	—	604M	98,304	—
Skip Transcoders [26]	38.4M	24,576	—	68.2M	32,768	—	272.7M	65,536	—	614M	98,304	—
MxDs	37.7M	3072	21,490	67.1M	4096	28,658	268.4M	8192	57,330	604M	8202	86,015

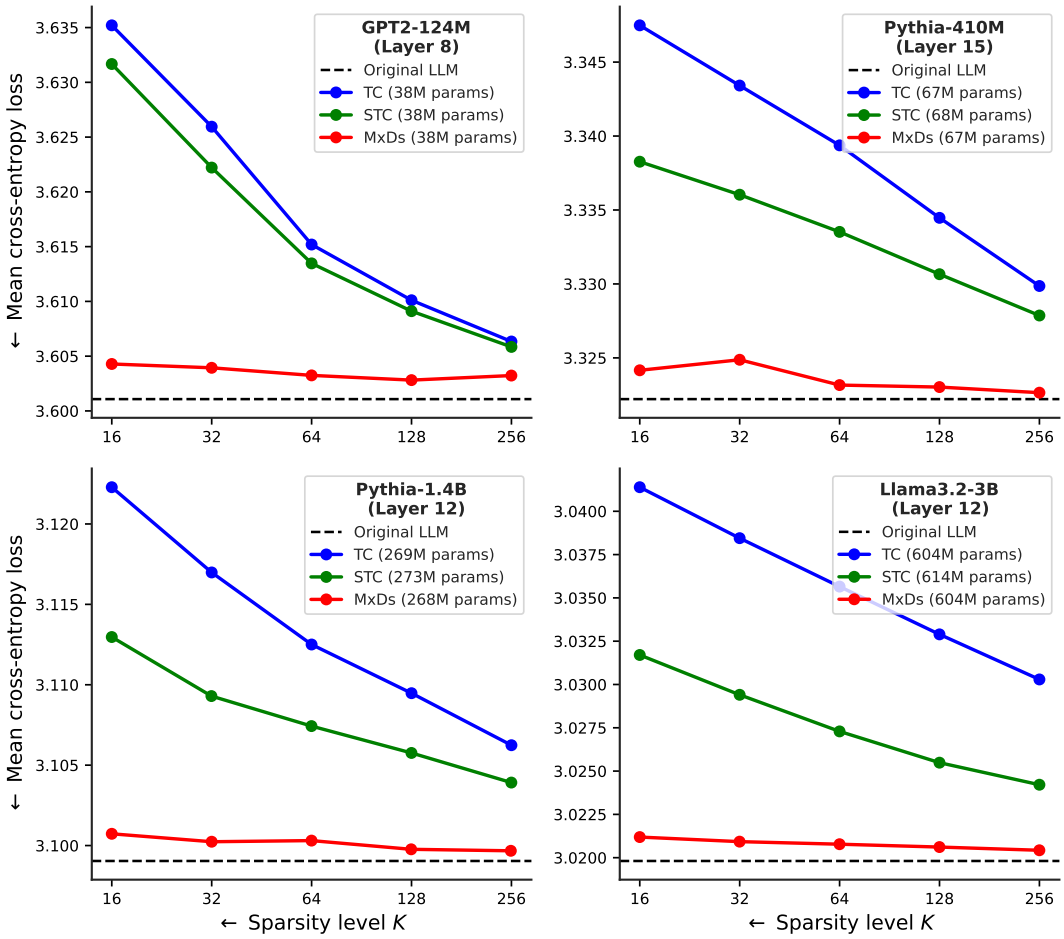

Figure 3: Model cross-entropy loss preserved when replacing MLPs with Transcoders [27], Skip Transcoders [26], and MxDs, as a function of the number of active units K (hidden neurons/experts). We highlight that MxDs have consistently lower loss at all levels of sparsity.

To compare with recent work [26], we adopt the `TopK` activation function [23] for sparsity-inducing function $\mathcal{S}(.)$, removing the need for an additional sparsity penalty.

3.1.1 Results: sparsity vs faithfulness

We train an exhaustive set of 60 sparse MLP approximations across 4 diverse LLMs with up to 3B parameters. We show in Figure 3 the resulting downstream base model cross-entropy loss when using the trained sparse layers in place of the original MLPs. As can be seen, not only do the proposed MxD layers outperform Transcoders [27] notably, but **model performance is similarly preserved at all sparsity levels in MxD layers**. With prior work finding sparse solutions to be more interpretable [17, 19], the performance gap of MxDs at small K is a significant advantage. Please also see Figure 10 for results with normalized MSE, where MxDs' reconstruction errors are up to an order of magnitude smaller. Full results on additional layers are included in Appendix B.3 for 48

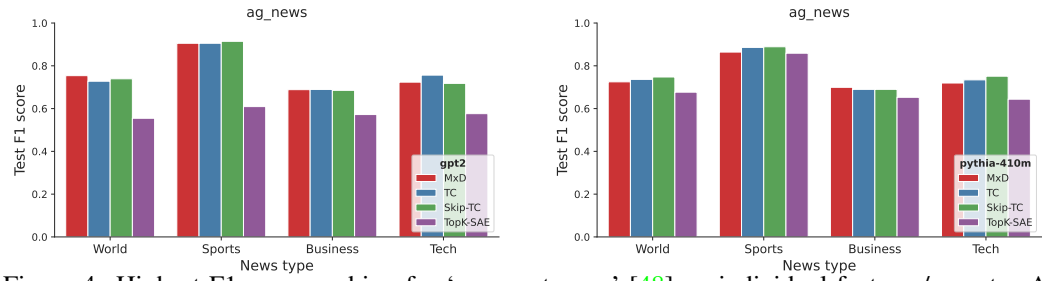

Figure 4: Highest F1 score probing for 'news category' [48] on individual features/experts. As expected, the MxDs remain competitive with the Transcoder baselines, outperforming TopK-SAEs.

more trained sparse layers. Please also see Appendix B.1 for qualitative and quantitative results for how faithfully the sparse layers propagate to the LLMs' output space of natural language.

The recent 'Skip Transcoders' (STCs) [26], introduce an additional IO parameters with a skip connection $\mathbf{S} \in \mathbb{R}^{I \times O}$ mapping the input directly to the output with $\mathbf{y} \approx \mathbf{D}^\top \mathbf{z} + \mathbf{S}^\top \mathbf{x}$. STC layers thus have considerably more parameters (e.g., STCs on `llama3.2-3B` have 10M more parameters than MxDs). Despite the smaller parameter counts, we find MxDs consistently outperform STCs on the sparsity-accuracy frontier, attesting to the benefits of MxDs' model form.

3.2 Feature evaluations

The accurate reconstruction of MxD models in Section 3.1 provides some evidence that MxDs are faithfully emulating the original MLP layers' functional mapping. However, for interpretability, we care equally about the extent to which the learned features correspond to specialized, human-interpretable concepts. We confirm that MxD's features compete with the baselines quantitatively in two ways: through probing for known concepts in Section 3.2.1 and by steering the model using the learned features Section 3.2.2. For all experiments in this section, we use the $K = 32$ models.

Shared experts and specialization Interestingly, we find MxDs naturally learn a 'shared' expert performing a common base transformation–the remaining $K - 1$ active experts are thus free to dedicate their capacity to modelling features unique to individual tokens. This emergent shared/private processing complements recent trends to use shared experts *by design* in MoEs [43, 44, 45, 46, 47] with [43] arguing this facilitates greater specialization. Furthermore, one may view the skip connection in STCs [26] as performing an analogous role to the shared expert. With MxDs, however, *all* units have the same high capacity to accurately learn separate subcomputation regardless of the frequency or rarity of features.

We also observe that our trained MxDs exhibit very few 'dead' experts, as shown in Appendix C.1, with many experts contributing actively. Furthermore, initial ablations in Appendix C.2 show that one can train MxDs without shared experts if desired, at small performance cost. Please see qualitative results of activated tokens for particular experts in Appendix E.

3.2.1 Sparse probing with individual features/experts

One challenge is that the sparse layers learn features in an unsupervised manner. As pointed out in [23], we therefore do not know which high-level features we ought to expect the model to learn (or even whether they exist in the OpenWebText training data). Nonetheless, we can reasonably expect a useful unsupervised model to learn at least a handful of commonly occurring concepts and linguistic themes. We accordingly focus our evaluation on the relative abilities of the sparse models to learn features well-predicting a variety of binary features used in the literature.

Concretely, to quantify the extent to which sparse layer features reliably fire in response to common high-level, interpretable concepts of natural language, we adopt the experimental settings of [49, 23, 19], training binary probes on the individual units of specialization (sparse hidden units z_n for TCs/SAEs and expert units a_n for MxDs–all pre-activation). For probing of sample-level concepts, we mean-pool activations across all non-padding tokens [19]. We train separate probes on 100 features with the largest mean difference between positive and negative activations, as per [49].

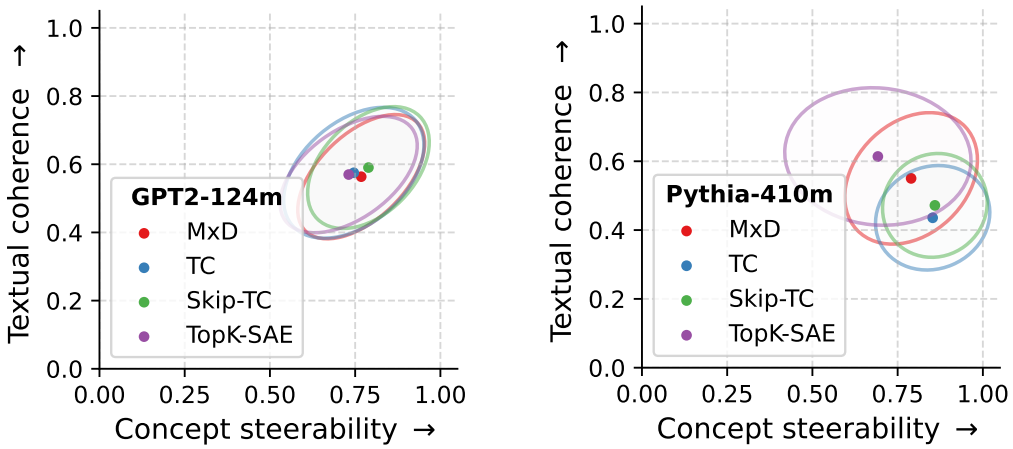

Figure 5: Mean score along dimensions of 'textual coherence' and 'steerability' of text generated by steering with the first 100 features of the sparse layers. Each sample is scored by 2 LLM judges.

We perform experiments on all 24 binary probing tasks in the SAEBench suite [19]. Four of which are shown in Figure 4, plotting the best F1 score (on a held-out set) for news topic classification in a 1-vs-all setting [48]. As can be seen, there exist individual MxD expert units that are predictive of various categories of news articles, competitive with the baselines. We refer readers to Appendix B.5 for additional experiments on 20 more sample-level probing tasks, 10 token-level probing tasks, and experimental details.

3.2.2 Feature steering

Specific features might reliably fire in response to interpretable patterns of the input, yet not contribute to the generation process. Here, we aim to test this functional role of features by steering the LLMs. We note that these experiments do not aim to establish TCs/MxDs as competitive with the SOTA for controllable LLM generation. Rather, we aim to validate that the learned features contribute mechanistically to the LLM's forward pass in a predictable way.

Mechanisms for steering Let $\lambda \in \mathbb{R}$ be a hyperparameter controlling the desired 'strength' of the model edit. For TCs, we hook the forward pass at the relevant layer to increase the presence of target feature n with $\hat{\mathbf{y}} = \mathbf{y} + \lambda \mathbf{d}_n$. In contrast, MxDs can be steered with $\hat{\mathbf{y}} = \mathbf{y} + \lambda \cdot (\mathbf{W}_n^\top \mathbf{z})$. Intuitively, increasing the weight of an expert's contribution in the forward pass modulates the token representation in the direction of the learned specialization.

Results We perform steering with the first 100 neurons/experts individually, using $\lambda := 100$ for all experiments. We generate a collection of 10 synthetic outputs for each neuron, each string consisting of 32 generated tokens to the prompt `'Let's talk about '`. We then ask two LLMs[2] to rate the collection of text along two dimensions separately: (1) the extent to which a shared concept, theme, or linguistic pattern is present throughout the generated collection of text, and (2) the grammatical fluency of the text (please see Appendix D.1 for the full prompt). As can be seen from the mean scores over the 100 neurons shown in Figure 5, MxDs are competitive with the baselines, exhibiting a similar trade-off between textual coherence and presence of concept as we expect.

4 Related work

Sparse decompositions Learning sparse [50, 25], non-negative [51] features of a data signal has found many applications in computer vision [15, 52, 53, 54] and natural language processing [55, 56, 57], motivated by the pursuit of interpretable, parts-based representations [13, 14]. In transformer-based language models [3], similar variants have been proposed for post-hoc analysis;

[2]We use `gemini-2.0-flash` and `llama-4-scout-17b-16e-instruct` as two independent LLM judges.

sparse autoencoders (SAEs) are a popular method that rewrites latent features as non-negative combinations of atoms in a learned overcomplete dictionary, imposing either soft sparsity penalties [6, 22, 31] or thresholding activations directly [23, 58, 59]. Recent work aims to sparsify the existing layers of pretrained LLMs, learning new MLPs with sparse hidden units [29] for circuit analysis [27] or more interpretable yet faithful computation [26, 60]. Despite the surge of interest in SAEs, many works are emerging drawing attention to their limitations–underperforming baselines for probing [61], unlearning [62], and steering [63], in addition to other pathologies [64, 32, 65, 66].

Conditional computation One natural alternative to static fully connected layers is conditional computation [67, 68]. Tracing back to the early work of [69, 70], single dense layers are replaced with specialized subunits–conditional on the input–as a form of layer-level sparsity. The Mixture of Experts (MoE) architecture [36, 71, 72] is a prominent example of conditional computation, breaking the link between parameter count and FLOPs. Consequently, MoEs have seen rapid adoption in SOTA models in recent years–scaling to very large parameter counts [73, 74, 75, 76, 77]. For parameter-efficient instruction tuning [37] introduces conditional $(\texttt{IA})^3$ adapters [38], modulating the MLP hidden dimension with the Hadamard product. Our proposed formulation with factorized weight tensors yields 'MoVs' [37] as a less scalable special case (see Appendix A.5). In contrast, MxDs model the decoder output space directly for reconstruction, and also provide significantly more specialized units than [37], making MxDs more suitable for our goal of interpretability.

Whilst the primary focus of MoEs has been on their impressive capabilities, the literature has observed that individual experts often specialize in particular semantic patterns of the input data, despite not being trained to do so [78, 79, 43, 80, 81]. For example, many works find that data that are in some sense similar are routed to the same experts–specializing to object shapes [82], texture [83], image category [84], or semantic patterns in natural language [36]. In the context of large language models, this emergent property of specialization in MoEs has been a primary focus of recent work: from encouraging monosemantic experts [85] or sparsity amongst experts' weights [86] to efficiently scaling the expert count for fine-grained specialization [40]. In contrast to these works exploring pre-training, we explore an efficient design of MoE to replace existing LLMs' dense layers.

5 Conclusion

In this paper, we showed the benefits of decomposing dense layers' computations as a mixture of interpretable sublayers. We proposed the Mixture of Decoders (MxD) layer to achieve this at scale, proving that MxDs' linear experts preserve the matrix rank properties of the original decoders. Experimentally, we showed MxDs significantly outperform on the sparsity-accuracy frontier when trained to replace dense MLP layers. Quantitative results on sparse probing and feature steering demonstrated MxDs nonetheless learn specialized latent features similarly to existing interpretability techniques. Crucially, MxDs reexamine the dominating neuron-level sparsity paradigm of popular techniques, providing evidence that specialization doesn't have to come with such a high cost to model performance. We believe MxDs (and specialization at the layer-level more generally) are an important step towards sparsity without sacrifice. We hope future work continues to build interpretable mechanisms that better preserve model capabilities.

Limitations Our experiments show MxDs outperform on the sparsity-accuracy frontier on 4 diverse LLMs. Whilst we fully anticipate this trend to continue in even larger models, our experiments only provide direct evidence for LLMs with up to 3B parameters, given our limited resources. Furthermore, whilst the `TopK` activation can greatly reduce the decoders' FLOPs, the large encoders in sparse MLPs and the gating function in MxDs remain an additional inference-time cost. Future work could explore hierarchical structures [85, 36] and/or efficient retrieval [87] for further reductions in FLOPs. Secondly, MoEs are prone to issues of expert imbalance [71], or collapse [88]. Just as a low learning rate helps prevent dead SAE features [89], we too find a low learning rate avoids dead experts (see Appendix C.1 exploring expert balance and Section 3.2.2 for functional diversity). Thus, similar care needs to be taken with MxDs' learning rate to ensure accurate yet non-degenerate reconstructions.

Acknowledgments

JO is grateful to Demian Till for reviewing the draft and providing valuable feedback and suggestions. JO would also like to thank Markos Georgopoulos, Benjamin Hayum, and Wisconsin AI Safety Initiative's Safety Scholars for insightful discussions throughout the project. We are also grateful to the open-source Zulip platform for facilitating research discussion.

References

[1] Abhimanyu Dubey, Abhinav Jauhri, Abhinav Pandey, Abhishek Kadian, Ahmad Al-Dahle, Aiesha Letman, Akhil Mathur, Alan Schelten, Amy Yang, Angela Fan, et al. The llama 3 herd of models. *arXiv preprint arXiv:2407.21783*, 2024.

[2] Morgane Riviere, Shreya Pathak, Pier Giuseppe Sessa, Cassidy Hardin, Surya Bhupatiraju, Léonard Hussenot, Thomas Mesnard, Bobak Shahriari, Alexandre Ramé, et al. Gemma 2: Improving open language models at a practical size. *arXiv preprint arXiv:2408.00118*, 2024.

[3] Alec Radford, Jeff Wu, Rewon Child, David Luan, Dario Amodei, and Ilya Sutskever. Language models are unsupervised multitask learners. 2019.

[4] Zhengxuan Wu, Atticus Geiger, Thomas Icard, Christopher Potts, and Noah Goodman. Interpretability at scale: Identifying causal mechanisms in alpaca. In A. Oh, T. Naumann, A. Globerson, K. Saenko, M. Hardt, and S. Levine, editors, *Adv. Neural Inform. Process. Syst. (NeurIPS)*, volume 36, pages 78205–78226. Curran Associates, Inc., 2023.

[5] Atticus Geiger, Zhengxuan Wu, Christopher Potts, Thomas Icard, and Noah Goodman. Finding alignments between interpretable causal variables and distributed neural representations. In Francesco Locatello and Vanessa Didelez, editors, *Proceedings of the Third Conference on Causal Learning and Reasoning*, volume 236 of *Proceedings of Machine Learning Research*, pages 160–187. PMLR, 01–03 Apr 2024.

[6] Adly Templeton. *Scaling monosemanticity: Extracting interpretable features from claude 3 sonnet*. Anthropic, 2024.

[7] Andy Arditi, Oscar Obeso, Aaquib Syed, Daniel Paleka, Nina Panickssery, Wes Gurnee, and Neel Nanda. Refusal in language models is mediated by a single direction. *arXiv preprint arXiv:2406.11717*, 2024.

[8] Collin Burns, Haotian Ye, Dan Klein, and Jacob Steinhardt. Discovering latent knowledge in language models without supervision. In *Int. Conf. Learn. Represent. (ICLR)*, 2023.

[9] David E. Rumelhart and James L. McClelland. *A General Framework for Parallel Distributed Processing*, pages 45–76. 1987.

[10] Geoffrey E Hinton. Distributed representations. 1984.

[11] Chris Olah, Nick Cammarata, Ludwig Schubert, Gabriel Goh, Michael Petrov, and Shan Carter. Zoom in: An introduction to circuits. *Distill*, 2020. doi: 10.23915/distill.00024.001. https://distill.pub/2020/circuits/zoom-in.

[12] Nelson Elhage, Tristan Hume, Catherine Olsson, Nicholas Schiefer, Tom Henighan, Shauna Kravec, Zac Hatfield-Dodds, Robert Lasenby, Dawn Drain, Carol Chen, Roger Grosse, Sam McCandlish, Jared Kaplan, Dario Amodei, Martin Wattenberg, and Christopher Olah. Toy models of superposition, 2022.

[13] Daniel D Lee and H Sebastian Seung. Learning the parts of objects by non-negative matrix factorization. *nature*, 401(6755):788–791, 1999.

[14] Bruno A Olshausen and David J Field. Emergence of simple-cell receptive field properties by learning a sparse code for natural images. *Nature*, 381(6583):607–609, 1996.

[15] Emmanuel J Candès, Xiaodong Li, Yi Ma, and John Wright. Robust principal component analysis? *Journal of the ACM (JACM)*, 58(3):1–37, 2011.

[16] Jiankang Deng, Jia Guo, Niannan Xue, and Stefanos Zafeiriou. Arcface: Additive angular margin loss for deep face recognition. In *IEEE Conf. Comput. Vis. Pattern Recog. (CVPR)*, pages 4690–4699, 2019.

[17] Vikram V. Ramaswamy, Sunnie S. Y. Kim, Ruth C. Fong, and Olga Russakovsky. Overlooked factors in concept-based explanations: Dataset choice, concept learnability, and human capability. *IEEE Conf. Comput. Vis. Pattern Recog. (CVPR)*, pages 10932–10941, 2022.

[18] Caden Juang, Gonçalo Paulo, Jacob Drori, and Nora Belrose. Open source automated interpretability for sparse autoencoder features. https://blog.eleuther.ai/autointerp/, July 2024. EleutherAI Blog.

[19] Adam Karvonen, Can Rager, Johnny Lin, Curt Tigges, Joseph Bloom, David Chanin, Callum McDougall, Yeu-Tong Lau, Eoin Farrell, Arthur Conmy, Kola Ayonrinde, Demian Till, Matthew Wearden, Samuel Marks, and Neel Nanda. SAEBench: A comprehensive benchmark for sparse autoencoders in language model interpretability. In *Int. Conf. Mach. Learn. (ICML)*, 2025.

[20] Zachary Chase Lipton. The mythos of model interpretability. *Communications of the ACM*, 61: 36 – 43, 2016.

[21] Forough Poursabzi-Sangdeh, Daniel G. Goldstein, Jake M. Hofman, Jennifer Wortman Vaughan, and Hanna M. Wallach. Manipulating and measuring model interpretability. *Proceedings of the 2021 CHI Conference on Human Factors in Computing Systems*, 2018.

[22] Robert Huben, Hoagy Cunningham, Logan Riggs Smith, Aidan Ewart, and Lee Sharkey. Sparse autoencoders find highly interpretable features in language models. In *Int. Conf. Learn. Represent. (ICLR)*, 2023.

[23] Leo Gao, Tom Dupre la Tour, Henk Tillman, Gabriel Goh, Rajan Troll, Alec Radford, Ilya Sutskever, Jan Leike, and Jeffrey Wu. Scaling and evaluating sparse autoencoders. In *Int. Conf. Learn. Represent. (ICLR)*, 2025.

[24] Bruno A Olshausen and David J Field. Sparse coding with an overcomplete basis set: A strategy employed by v1? *Vision research*, 37(23):3311–3325, 1997.

[25] M. Aharon, M. Elad, and A. Bruckstein. K-svd: An algorithm for designing overcomplete dictionaries for sparse representation. *IEEE Transactions on Signal Processing*, 54(11):4311–4322, 2006. doi: 10.1109/TSP.2006.881199.

[26] Gonçalo Paulo, Stepan Shabalin, and Nora Belrose. Transcoders beat sparse autoencoders for interpretability. *arXiv preprint arXiv:2501.18823*, 2025.

[27] Jacob Dunefsky, Philippe Chlenski, and Neel Nanda. Transcoders find interpretable LLM feature circuits. In *Adv. Neural Inform. Process. Syst. (NeurIPS)*, 2024.

[28] Lee Sharkey, Bilal Chughtai, Joshua Batson, Jack Lindsey, Jeff Wu, Lucius Bushnaq, Nicholas Goldowsky-Dill, Stefan Heimersheim, Alejandro Ortega, Joseph Bloom, et al. Open problems in mechanistic interpretability. *arXiv preprint arXiv:2501.16496*, 2025.

[29] Trenton Bricken, Adly Templeton, Joshua Batson, Brian Chen, Adam Jermyn, Tom Conerly, Nick Turner, Cem Anil, Carson Denison, Amanda Askell, Robert Lasenby, Yifan Wu, Shauna Kravec, Nicholas Schiefer, Tim Maxwell, Nicholas Joseph, Zac Hatfield-Dodds, Alex Tamkin, Karina Nguyen, Brayden McLean, Josiah E Burke, Tristan Hume, Shan Carter, Tom Henighan, and Christopher Olah. Towards monosemanticity: Decomposing language models with dictionary learning. *Transformer Circuits Thread*, 2023. https://transformer-circuits.pub/2023/monosemantic-features/index.html.

[30] Samuel Marks, Adam Karvonen, and Aaron Mueller. dictionary_learning. https://github.com/saprmarks/dictionary_learning, 2024.

[31] Senthooran Rajamanoharan, Tom Lieberum, Nicolas Sonnerat, Arthur Conmy, Vikrant Varma, János Kramár, and Neel Nanda. Jumping ahead: Improving reconstruction fidelity with jumprelu sparse autoencoders. *arXiv preprint arXiv:2407.14435*, 2024.

[32] Joshua Engels, Logan Riggs, and Max Tegmark. Decomposing the dark matter of sparse autoencoders. *arXiv preprint arXiv:2410.14670*, 2024.

[33] Noam Shazeer. Glu variants improve transformer. *arXiv preprint arXiv:2002.05202*, 2020.

[34] Tamara G Kolda and Brett W Bader. Tensor decompositions and applications. *SIAM review*, 51 (3):455–500, 2009.

[35] Grigorios G Chrysos, Yongtao Wu, Razvan Pascanu, Philip Torr, and Volkan Cevher. Hadamard product in deep learning: Introduction, advances and challenges. *IEEE Transactions on Pattern Analysis and Machine Intelligence*, pages 1–20, 2025. doi: 10.1109/TPAMI.2025.3560423.

[36] Noam Shazeer, *Azalia Mirhoseini, *Krzysztof Maziarz, Andy Davis, Quoc Le, Geoffrey Hinton, and Jeff Dean. Outrageously large neural networks: The sparsely-gated mixture-of-experts layer. In *Int. Conf. Learn. Represent. (ICLR)*, 2017.

[37] Ted Zadouri, Ahmet Üstün, Arash Ahmadian, Beyza Ermis, Acyr Locatelli, and Sara Hooker. Pushing mixture of experts to the limit: Extremely parameter efficient moe for instruction tuning. In *Int. Conf. Learn. Represent. (ICLR)*, 2024.

[38] Haokun Liu, Derek Tam, Muqeeth Mohammed, Jay Mohta, Tenghao Huang, Mohit Bansal, and Colin Raffel. Few-shot parameter-efficient fine-tuning is better and cheaper than in-context learning. In Alice H. Oh, Alekh Agarwal, Danielle Belgrave, and Kyunghyun Cho, editors, *Adv. Neural Inform. Process. Syst. (NeurIPS)*, 2022.

[39] Dan Hendrycks and Kevin Gimpel. Gaussian error linear units (gelus). *arXiv preprint arXiv:1606.08415*, 2016.

[40] James Oldfield, Markos Georgopoulos, Grigorios Chrysos, Christos Tzelepis, Yannis Panagakis, Mihalis Nicolaou, Jiankang Deng, and Ioannis Patras. Multilinear mixture of experts: Scalable expert specialization through factorization. In *Adv. Neural Inform. Process. Syst. (NeurIPS)*, 2024.

[41] Stella Biderman, Hailey Schoelkopf, Quentin Gregory Anthony, Herbie Bradley, Kyle O'Brien, Eric Hallahan, Mohammad Aflah Khan, Shivanshu Purohit, USVSN Sai Prashanth, Edward Raff, et al. Pythia: A suite for analyzing large language models across training and scaling. In *Int. Conf. Mach. Learn. (ICML)*, pages 2397–2430. PMLR, 2023.

[42] Aaron Gokaslan, Vanya Cohen, Ellie Pavlick, and Stefanie Tellex. Openwebtext corpus. http://Skylion007.github.io/OpenWebTextCorpus, 2019.

[43] Damai Dai, Chengqi Deng, Chenggang Zhao, R. X. Xu, Huazuo Gao, Deli Chen, Jiashi Li, Wangding Zeng, Xingkai Yu, Y. Wu, Zhenda Xie, Y. K. Li, Panpan Huang, Fuli Luo, Chong Ruan, Zhifang Sui, and Wenfeng Liang. Deepseekmoe: Towards ultimate expert specialization in mixture-of-experts language models, 2024.

[44] Meta AI. The llama 4 herd: The beginning of a new era of natively multimodal ai innovation, 2025. URL https://ai.meta.com/blog/llama-4-multimodal-intelligence/. Accessed: 2025-04-06.

[45] Qwen Team. Qwen1.5-moe: Matching 7b model performance with 1/3 activated parameters", February 2024. URL https://qwenlm.github.io/blog/qwen-moe/.

[46] An Yang, Baosong Yang, Binyuan Hui, Bo Zheng, Bowen Yu, Chang Zhou, Chengpeng Li, Chengyuan Li, Dayiheng Liu, Fei Huang, Guanting Dong, Haoran Wei, Huan Lin, Jialong Tang, Jialin Wang, Jian Yang, Jianhong Tu, Jianwei Zhang, Jianxin Ma, Jianxin Yang, Jin Xu, Jingren Zhou, Jinze Bai, Jinzheng He, Junyang Lin, Kai Dang, Keming Lu, Keqin Chen, Kexin Yang, Mei Li, Mingfeng Xue, Na Ni, Pei Zhang, Peng Wang, Ru Peng, Rui Men, Ruize Gao, Runji Lin, Shijie Wang, Shuai Bai, Sinan Tan, Tianhang Zhu, Tianhao Li, Tianyu Liu, Wenbin Ge, Xiaodong Deng, Xiaohuan Zhou, Xingzhang Ren, Xinyu Zhang, Xipin Wei, Xuancheng Ren, Xuejing Liu, Yang Fan, Yang Yao, Yichang Zhang, Yu Wan, Yunfei Chu, Yuqiong Liu, Zeyu Cui, Zhenru Zhang, Zhifang Guo, and Zhihao Fan. Qwen2 technical report, 2024.

[47] An Yang, Bowen Yu, Chengyuan Li, Dayiheng Liu, Fei Huang, Haoyan Huang, Jiandong Jiang, Jianhong Tu, Jianwei Zhang, Jingren Zhou, Junyang Lin, Kai Dang, Kexin Yang, Le Yu, Mei Li, Minmin Sun, Qin Zhu, Rui Men, Tao He, Weijia Xu, Wenbiao Yin, Wenyuan Yu, Xiafei Qiu, Xingzhang Ren, Xinlong Yang, Yong Li, Zhiying Xu, and Zipeng Zhang. Qwen2.5-1m technical report, 2025.

[48] Antonio Gulli. Ag corpus of news articles. http://groups.di.unipi.it/~gulli/AG_corpus_of_news_articles.html, 2005.

[49] Wes Gurnee, Neel Nanda, Matthew Pauly, Katherine Harvey, Dmitrii Troitskii, and Dimitris Bertsimas. Finding neurons in a haystack: Case studies with sparse probing. *Transactions on Machine Learning Research*, 2023. ISSN 2835-8856.

[50] Rodolphe Jenatton, Guillaume Obozinski, and Francis Bach. Structured sparse principal component analysis. In Yee Whye Teh and Mike Titterington, editors, *Proceedings of the Thirteenth International Conference on Artificial Intelligence and Statistics*, volume 9 of *Proceedings of Machine Learning Research*, pages 366–373, Chia Laguna Resort, Sardinia, Italy, 13–15 May 2010. PMLR.

[51] Patrik O Hoyer. Non-negative matrix factorization with sparseness constraints. *Journal of machine learning research*, 5(Nov):1457–1469, 2004.

[52] Edo Collins, Radhakrishna Achanta, and Sabine Süsstrunk. *Deep Feature Factorization for Concept Discovery*, page 352–368. Springer International Publishing, 2018. ISBN 9783030012649. doi: 10.1007/978-3-030-01264-9_21.

[53] James Oldfield, Christos Tzelepis, Yannis Panagakis, Mihalis Nicolaou, and Ioannis Patras. Panda: Unsupervised learning of parts and appearances in the feature maps of GANs. In *Int. Conf. Learn. Represent. (ICLR)*, 2023.

[54] Yue Song, Thomas Anderson Keller, Yisong Yue, Pietro Perona, and Max Welling. Unsupervised representation learning from sparse transformation analysis, 2024.

[55] Wei Xu, Xin Liu, and Yihong Gong. Document clustering based on non-negative matrix factorization. In *Proceedings of the 26th Annual International ACM SIGIR Conference on Research and Development in Informaion Retrieval*, SIGIR '03, page 267–273, New York, NY, USA, 2003. Association for Computing Machinery. ISBN 1581136463. doi: 10.1145/860435.860485.

[56] Da Kuang, Jaegul Choo, and Haesun Park. Nonnegative matrix factorization for interactive topic modeling and document clustering. *Partitional clustering algorithms*, pages 215–243, 2015.

[57] Sanjeev Arora, Yuanzhi Li, Yingyu Liang, Tengyu Ma, and Andrej Risteski. Linear algebraic structure of word senses, with applications to polysemy. *Transactions of the Association for Computational Linguistics*, 6:483–495, 2018. doi: 10.1162/tacl_a_00034.

[58] Alireza Makhzani and Brendan Frey. K-sparse autoencoders. *arXiv preprint arXiv:1312.5663*, 2013.

[59] Bart Bussmann, Patrick Leask, and Neel Nanda. Batchtopk sparse autoencoders. In *NeurIPS 2024 Workshop on Scientific Methods for Understanding Deep Learning*, 2024.

[60] Lucy Farnik, Tim Lawson, Conor Houghton, and Laurence Aitchison. Jacobian sparse autoencoders: Sparsify computations, not just activations, 2025.

[61] Subhash Kantamneni, Joshua Engels, Senthooran Rajamanoharan, Max Tegmark, and Neel Nanda. Are sparse autoencoders useful? a case study in sparse probing, 2025.

[62] Eoin Farrell, Yeu-Tong Lau, and Arthur Conmy. Applying sparse autoencoders to unlearn knowledge in language models, 2024.

[63] Zhengxuan Wu, Aryaman Arora, Atticus Geiger, Zheng Wang, Jing Huang, Dan Jurafsky, Christopher D. Manning, and Christopher Potts. AxBench: Steering LLMs? even simple baselines outperform sparse autoencoders. In *Int. Conf. Mach. Learn. (ICML)*, 2025.

[64] David Chanin, James Wilken-Smith, Tomáš Dulka, Hardik Bhatnagar, and Joseph Bloom. A is for absorption: Studying feature splitting and absorption in sparse autoencoders, 2024.

[65] Patrick Leask, Bart Bussmann, Michael Pearce, Joseph Bloom, Curt Tigges, Noura Al Moubayed, Lee Sharkey, and Neel Nanda. Sparse autoencoders do not find canonical units of analysis, 2025.

[66] Gonçalo Paulo and Nora Belrose. Sparse autoencoders trained on the same data learn different features, 2025.

[67] Yizeng Han, Gao Huang, Shiji Song, Le Yang, Honghui Wang, and Yulin Wang. Dynamic neural networks: A survey. *IEEE Trans. Pattern Anal. Mach. Intell. (TPAMI)*, 44(11):7436–7456, 2021.

[68] Emmanuel Bengio, Pierre-Luc Bacon, Joelle Pineau, and Doina Precup. Conditional computation in neural networks for faster models. In *Int. Conf. Mach. Learn. Worksh. (ICMLW)*, 2015.

[69] Robert A Jacobs, Michael I Jordan, and Andrew G Barto. Task decomposition through competition in a modular connectionist architecture: The what and where vision tasks. *Cognitive science*, 15(2):219–250, 1991.

[70] Robert A Jacobs, Michael I Jordan, Steven J Nowlan, and Geoffrey E Hinton. Adaptive mixtures of local experts. *Neural computation*, 3(1):79–87, 1991.

[71] William Fedus, Barret Zoph, and Noam Shazeer. Switch transformers: Scaling to trillion parameter models with simple and efficient sparsity. *Journal of Machine Learning Research*, 23 (120):1–39, 2022.

[72] Barret Zoph, Irwan Bello, Sameer Kumar, Nan Du, Yanping Huang, Jeff Dean, Noam Shazeer, and William Fedus. St-moe: Designing stable and transferable sparse expert models. *arXiv preprint arXiv:2202.08906*, 2022.

[73] Dmitry Lepikhin, HyoukJoong Lee, Yuanzhong Xu, Dehao Chen, Orhan Firat, Yanping Huang, Maxim Krikun, Noam Shazeer, and Zhifeng Chen. GShard: Scaling giant models with conditional computation and automatic sharding. In *Int. Conf. Learn. Represent. (ICLR)*, 2021.

[74] Nan Du, Yanping Huang, Andrew M Dai, Simon Tong, Dmitry Lepikhin, Yuanzhong Xu, Maxim Krikun, Yanqi Zhou, Adams Wei Yu, Orhan Firat, et al. Glam: Efficient scaling of language models with mixture-of-experts. In *Int. Conf. Mach. Learn. (ICML)*, pages 5547–5569. PMLR, 2022.

[75] Albert Q. Jiang, Alexandre Sablayrolles, Antoine Roux, Arthur Mensch, Blanche Savary, Chris Bamford, Devendra Singh Chaplot, Diego de las Casas, Emma Bou Hanna, Florian Bressand, Gianna Lengyel, Guillaume Bour, Guillaume Lample, Lélio Renard Lavaud, Lucile Saulnier, Marie-Anne Lachaux, Pierre Stock, Sandeep Subramanian, Sophia Yang, Szymon Antoniak, Teven Le Scao, Théophile Gervet, Thibaut Lavril, Thomas Wang, Timothée Lacroix, and William El Sayed. Mixtral of experts, 2024.

[76] DeepSeek-AI, Aixin Liu, Bei Feng, Bing Xue, Bingxuan Wang, Bochao Wu, Chengda Lu, Chenggang Zhao, Chengqi Deng, Chenyu Zhang, Chong Ruan, Damai Dai, Daya Guo, Dejian Yang, Deli Chen, Dongjie Ji, Erhang Li, Fangyun Lin, Fucong Dai, Fuli Luo, Guangbo Hao, Guanting Chen, Guowei Li, H. Zhang, Han Bao, Hanwei Xu, Haocheng Wang, Haowei Zhang, Honghui Ding, Huajian Xin, Huazuo Gao, Hui Li, Hui Qu, J. L. Cai, Jian Liang, Jianzhong Guo, Jiaqi Ni, Jiashi Li, Jiawei Wang, Jin Chen, Jingchang Chen, Jingyang Yuan, Junjie Qiu, Junlong Li, Junxiao Song, Kai Dong, Kai Hu, Kaige Gao, Kang Guan, Kexin Huang, Kuai Yu, Lean Wang, Lecong Zhang, Lei Xu, Leyi Xia, Liang Zhao, Litong Wang, Liyue Zhang, Meng Li, Miaojun Wang, Mingchuan Zhang, Minghua Zhang, Minghui Tang, Mingming Li, Ning Tian, Panpan Huang, Peiyi Wang, Peng Zhang, Qiancheng Wang, Qihao Zhu, Qinyu Chen, Qiushi Du, R. J. Chen, R. L. Jin, Ruiqi Ge, Ruisong Zhang, Ruizhe Pan, Runji Wang, Runxin Xu, Ruoyu Zhang, Ruyi Chen, S. S. Li, Shanghao Lu, Shangyan Zhou, Shanhuang Chen, Shaoqing Wu, Shengfeng Ye, Shengfeng Ye, Shirong Ma, Shiyu Wang, Shuang Zhou, Shuiping Yu, Shunfeng Zhou, Shuting Pan, T. Wang, Tao Yun, Tian Pei, Tianyu Sun, W. L. Xiao, Wangding Zeng, Wanjia Zhao, Wei An, Wen Liu, Wenfeng Liang, Wenjun Gao, Wenqin Yu, Wentao Zhang, X. Q. Li, Xiangyue Jin, Xianzu Wang, Xiao Bi, Xiaodong Liu, Xiaohan Wang, Xiaojin Shen, Xiaokang Chen, Xiaokang Zhang, Xiaosha Chen, Xiaotao Nie, Xiaowen Sun, Xiaoxiang Wang, Xin Cheng, Xin Liu, Xin Xie, Xingchao Liu, Xingkai Yu, Xinnan Song, Xinxia Shan, Xinyi Zhou, Xinyu Yang, Xinyuan Li, Xuecheng Su, Xuheng Lin, Y. K. Li, Y. Q. Wang, Y. X. Wei, Y. X. Zhu, Yang Zhang, Yanhong Xu, Yanhong Xu, Yanping Huang, Yao Li, Yao Zhao, Yaofeng Sun, Yaohui Li, Yaohui Wang, Yi Yu, Yi Zheng, Yichao Zhang, Yifan Shi, Yiliang Xiong, Ying He, Ying Tang, Yishi Piao, Yisong Wang, Yixuan Tan, Yiyang Ma, Yiyuan Liu, Yongqiang Guo, Yu Wu, Yuan Ou, Yuchen Zhu, Yuduan Wang, Yue Gong, Yuheng Zou, Yujia He, Yukun Zha, Yunfan Xiong, Yunxian Ma, Yuting Yan, Yuxiang Luo, Yuxiang You, Yuxuan Liu, Yuyang Zhou, Z. F. Wu, Z. Z. Ren, Zehui Ren, Zhangli Sha, Zhe Fu, Zhean Xu, Zhen Huang, Zhen Zhang, Zhenda Xie, Zhengyan Zhang, Zhewen Hao, Zhibin Gou, Zhicheng Ma, Zhigang Yan, Zhihong Shao, Zhipeng Xu, Zhiyu Wu, Zhongyu Zhang, Zhuoshu Li, Zihui Gu, Zijia Zhu, Zijun Liu, Zilin Li, Ziwei Xie, Ziyang Song, Ziyi Gao, and Zizheng Pan. Deepseek-v3 technical report, 2025.

[77] Joan Puigcerver, Carlos Riquelme, Basil Mustafa, and Neil Houlsby. From sparse to soft mixtures of experts. In *Int. Conf. Learn. Represent. (ICLR)*, 2024.

[78] Aya Abdelsalam Ismail, Sercan O Arik, Jinsung Yoon, Ankur Taly, Soheil Feizi, and Tomas Pfister. Interpretable mixture of experts. *Transactions on Machine Learning Research*, 2023. ISSN 2835-8856.

[79] Marmik Chaudhari, Idhant Gulati, Nishkal Hundia, Pranav Karra, and Shivam Raval. Moe lens - an expert is all you need. In *Sparsity in LLMs (SLLM): Deep Dive into Mixture of Experts, Quantization, Hardware, and Inference*, 2025.

[80] Huy Nguyen, Xing Han, Carl Harris, Suchi Saria, and Nhat Ho. On expert estimation in hierarchical mixture of experts: Beyond softmax gating functions, 2025.

[81] Stefan Nielsen, Rachel Teo, Laziz Abdullaev, and Tan Minh Nguyen. Tight clusters make specialized experts. In *Int. Conf. Learn. Represent. (ICLR)*, 2025.

[82] Brandon Yang, Gabriel Bender, Quoc V Le, and Jiquan Ngiam. Condconv: Conditionally parameterized convolutions for efficient inference. *Adv. Neural Inform. Process. Syst. (NeurIPS)*, 32, 2019.

[83] Basil Mustafa, Carlos Riquelme Ruiz, Joan Puigcerver, Rodolphe Jenatton, and Neil Houlsby. Multimodal contrastive learning with LIMoe: the language-image mixture of experts. In Alice H. Oh, Alekh Agarwal, Danielle Belgrave, and Kyunghyun Cho, editors, *Adv. Neural Inform. Process. Syst. (NeurIPS)*, 2022.

[84] Carlos Riquelme, Joan Puigcerver, Basil Mustafa, Maxim Neumann, Rodolphe Jenatton, André Susano Pinto, Daniel Keysers, and Neil Houlsby. Scaling vision with sparse mixture of experts. *Adv. Neural Inform. Process. Syst. (NeurIPS)*, 34:8583–8595, 2021.

[85] Jungwoo Park, Ahn Young Jin, Kee-Eung Kim, and Jaewoo Kang. Monet: Mixture of monosemantic experts for transformers. In *Int. Conf. Learn. Represent. (ICLR)*, 2025.

[86] Xingyi Yang, Constantin Venhoff, Ashkan Khakzar, Christian Schroeder de Witt, Puneet K. Dokania, Adel Bibi, and Philip Torr. Mixture of experts made intrinsically interpretable, 2025.

[87] Xu Owen He. Mixture of a million experts, 2024.

[88] Zewen Chi, Li Dong, Shaohan Huang, Damai Dai, Shuming Ma, Barun Patra, Saksham Singhal, Payal Bajaj, Xia Song, Xian-Ling Mao, Heyan Huang, and Furu Wei. On the representation collapse of sparse mixture of experts. In Alice H. Oh, Alekh Agarwal, Danielle Belgrave, and Kyunghyun Cho, editors, *Adv. Neural Inform. Process. Syst. (NeurIPS)*, 2022.

[89] Arthur Conmy. My best guess at the important tricks for training 1l saes. https://www.lesswrong.com/posts/fifPCos6ddsmJYahD/my-best-guess-at-the-important-tricks-for-training-1l-saes, December 2023. LessWrong.

[90] James E. Gentle. *Matrix Algebra: Theory, Computations, and Applications in Statistics*. Springer, New York, 2nd edition, 2007.

[91] Nicholas D Sidiropoulos and Rasmus Bro. On the uniqueness of multilinear decomposition of n-way arrays. *Journal of Chemometrics: A Journal of the Chemometrics Society*, 14(3): 229–239, 2000.

[92] Donghyun Lee, Jaeyong Lee, Genghan Zhang, Mo Tiwari, and Azalia Mirhoseini. CATS: Context-aware thresholding for sparsity in large language models. In *First Conference on Language Modeling*, 2024.

[93] Frank Lauren Hitchcock. The expression of a tensor or a polyadic as a sum of products. *Journal of Mathematics and Physics*, 6:164–189, 1927.

[94] J. Douglas Carroll and Jih Jie Chang. Analysis of individual differences in multidimensional scaling via an n-way generalization of "eckart-young" decomposition. *Psychometrika*, 35: 283–319, 1970.

[95] CodeParrot. Github code dataset. https://huggingface.co/datasets/codeparrot/github-code, 2022.

[96] Yupeng Hou, Jiacheng Li, Zhankui He, An Yan, Xiusi Chen, and Julian McAuley. Bridging language and items for retrieval and recommendation. *arXiv preprint arXiv:2403.03952*, 2024.

[97] Philipp Koehn. Europarl: A parallel corpus for statistical machine translation. In *Proceedings of Machine Translation Summit X: Papers*, pages 79–86, Phuket, Thailand, September 13-15 2005.

[98] Maria De-Arteaga, Alexey Romanov, Hanna Wallach, Jennifer Chayes, Christian Borgs, Alexandra Chouldechova, Sahin Geyik, Krishnaram Kenthapadi, and Adam Tauman Kalai. Bias in bios: A case study of semantic representation bias in a high-stakes setting. In *Proceedings of the Conference on Fairness, Accountability, and Transparency*, FAT* '19, page 120–128, New York, NY, USA, 2019. Association for Computing Machinery. ISBN 9781450361255. doi: 10.1145/3287560.3287572. URL https://doi.org/10.1145/3287560.3287572.

[99] Anthony Duong Joseph Bloom, Curt Tigges and David Chanin. Saelens. https://github.com/jbloomAus/SAELens, 2024.

Appendix

Table of Contents

A Proofs and additional technical results

A.1 Proof of rank equality

Proof of Lemma 1. We first derive the expression for expert n's weight matrix $\mathbf{W}_n = \mathbf{D}\,\mathrm{diag}(\mathbf{c}_n) \in \mathbb{R}^{H\times O}$ and then show the rank equality that follows. First, recall that we have the third-order weight tensor defined as

$$\boldsymbol{\mathcal{W}}(n,h,:) = \mathbf{c}_n * \mathbf{d}_h \in \mathbb{R}^O,$$

for matrices $\mathbf{C} \in \mathbb{R}^{N\times O}$, $\mathbf{D} \in \mathbb{R}^{H\times O}$. We can express each element of the tensor $\boldsymbol{\mathcal{W}} \in \mathbb{R}^{N\times H\times O}$ in terms of elements of the two matrices as

$$\boldsymbol{\mathcal{W}}(n,h,o) = c_{no}\cdot d_{ho} = (\mathbf{D})_{ho}\cdot c_{no}. \tag{6}$$

Equation (6) shows that for a fixed expert n, the n^{th} row $\mathbf{c}_n \in \mathbb{R}^O$ essentially scales the columns of matrix $\mathbf{D} \in \mathbb{R}^{H\times O}$. This is equivalent to right-multiplying matrix $\mathbf{D}$ by a diagonal matrix formed from $\mathbf{c}_n \in \mathbb{R}^O$. Indeed, the (h,o) entry of such matrix product is

$$[\mathbf{D}\,\mathrm{diag}(\mathbf{c}_n)]_{ho} = \sum_{i=1}^{O} (\mathbf{D})_{hi}\,\mathrm{diag}(\mathbf{c}_n)_{io} \tag{7}$$

$$= (\mathbf{D})_{ho}\,\mathrm{diag}(\mathbf{c}_n)_{oo} \tag{8}$$

$$= d_{ho}\cdot c_{no}, \tag{9}$$

since all off-diagonal terms (i.e., $i \neq o$) in Equation (7) vanish and $\text{diag}(\mathbf{c}_n)_{oo} = c_{no}$ by construction. Comparing Equation (6) and Equation (9) shows that, for every $h \in \{1, 2, \ldots, H\}$ and $o \in \{1, 2, \ldots, O\}$ we have

$$\boldsymbol{\mathcal{W}}(n, h, o) = [\mathbf{D}\,\text{diag}(\mathbf{c}_n)]_{ho}\,.$$

Hence, indexing into the first mode of the tensor alone gives us the matrix-valued expression for expert n as claimed:

$$\boldsymbol{\mathcal{W}}(n, :, :) = \mathbf{W}_n = \mathbf{D}\,\text{diag}(\mathbf{c}_n) \in \mathbb{R}^{H \times O}.$$

Finally, a standard result in linear algebra [90] has that $\text{rank}(\mathbf{AB}) = \text{rank}(\mathbf{A})$ for any $\mathbf{A} \in \mathbb{R}^{H \times O}$ and invertible matrix $\mathbf{B} \in \mathbb{R}^{O \times O}$. Since matrix $\text{diag}\,(\mathbf{c}_n) \in \mathbb{R}^{O \times O}$ is invertible by assumption in Lemma 1, setting $\mathbf{A} = \mathbf{D}$ and $\mathbf{B} = \text{diag}(\mathbf{c}_n)$ yields the rank equality. □

A.2 Proof of MxD forward pass equivalence

Recall we have input vector $\mathbf{z} \in \mathbb{R}^H$, expert coefficients $\mathbf{a} \in \mathbb{R}^N$, and layer weights $\boldsymbol{\mathcal{W}} \in \mathbb{R}^{N \times H \times O}$. The weights are defined in Equation (4) element-wise through the Hadamard product $*$ as

$$\boldsymbol{\mathcal{W}}(n, h, :) = \mathbf{c}_n * \mathbf{d}_h \in \mathbb{R}^O, \quad \forall\, n \in \{1, \ldots, N\},\ h \in \{1, \ldots, H\},$$

for learnable parameters $\mathbf{C} \in \mathbb{R}^{N \times O}$, $\mathbf{D} \in \mathbb{R}^{H \times O}$. Lemma 2 states that MxD's forward pass can be equivalently expressed as

$$\sum_{n=1}^{N} a_n \big(\mathbf{W}_n^\top \mathbf{z}\big) = \big(\mathbf{C}^\top \mathbf{a}\big) \;*\; \big(\mathbf{D}^\top \mathbf{z}\big).$$

Proof of Lemma 2. The LHS can first be re-written as an explicit sum over the hidden dimension

$$\hat{\mathbf{y}} = \sum_{n=1}^{N} a_n \big(\mathbf{W}_n^\top \mathbf{z}\big) = \sum_{n=1}^{N} \sum_{h=1}^{H} a_n \big(\mathbf{w}_{nh:} z_h\big) \in \mathbb{R}^O. \tag{10}$$

Plugging in the definition of $\mathbf{w}_{nh:} \in \mathbb{R}^O$ from Equation (4) then yields

$$\begin{aligned}
\hat{\mathbf{y}} &= \sum_{n=1}^{N} \sum_{h=1}^{H} a_n \big(\mathbf{w}_{nh:} z_h\big) && (11)\\
&= \sum_{n=1}^{N} \sum_{h=1}^{H} a_n \big(\,(\mathbf{c}_n * \mathbf{d}_h)\, z_h\big) && (12)\\
&= \left(\sum_{n=1}^{N} a_n \mathbf{c}_n\right) * \left(\sum_{h=1}^{H} z_h \mathbf{d}_h\right) && (13)\\
&= \big(\mathbf{C}^\top \mathbf{a}\big) * \big(\mathbf{D}^\top \mathbf{z}\big), && (14)
\end{aligned}$$

which is exactly the RHS of Equation (5), showing the MxD forward pass is equivalent to the Hadamard product of $\mathbf{C}^\top \mathbf{a}$ and $\mathbf{D}^\top \mathbf{z}$. □

A.3 Intuition for weight parameterization through the lens of tensor methods

A second complementary way of viewing the MxD layer's parameterization (and its full-rank properties) is through the lens of tensor methods [34]. A tensor-based motivation for MxD's weight tensor parameterization and forward pass is presented in Appendix A.3.1 and Appendix A.3.2, respectively.

Notation and definitions A brief primer is first included below, based on [34] (and can be safely skipped for those already familiar):

- The **mode-n fibers** of an N^{th} order tensor $\boldsymbol{\mathcal{X}} \in \mathbb{R}^{I_1 \times I_2 \times \cdots \times I_N}$ are the I_n-dimensional column vectors obtained by fixing every index except that of the n^{th} mode (e.g., $\mathbf{x}_{:i_2 i_3} \in \mathbb{R}^{I_1}$ are the mode-1 fibers of a third-order tensor $\boldsymbol{\mathcal{X}} \in \mathbb{R}^{I_1 \times I_2 \times I_3}$). Stacking all mode-$n$ fibers column-wise yields the so-called **mode-n unfolding** $\mathbf{X}_{(n)} \in \mathbb{R}^{I_n \times \bar{I}_n}$, with number of columns given by the product of remaining dimensions $\bar{I}_n = \prod_{\substack{t=1 \\ t \neq n}}^{N} I_t$.
- The **Khatri-Rao product** (denoted by $\odot$) between two matrices $\mathbf{A} \in \mathbb{R}^{I \times K}$ and $\mathbf{B} \in \mathbb{R}^{J \times K}$, is the column-wise Kronecker product (denoted by $\otimes$): $\mathbf{A} \odot \mathbf{B} := \begin{bmatrix} \mathbf{a}_{:1} \otimes \mathbf{b}_{:1} & \cdots & \mathbf{a}_{:K} \otimes \mathbf{b}_{:K} \end{bmatrix} \in \mathbb{R}^{(I \cdot J) \times K}$.
- The **mode-n (vector) product** of a tensor $\boldsymbol{\mathcal{X}} \in \mathbb{R}^{I_1 \times I_2 \times \cdots \times I_N}$ with a vector $\mathbf{u} \in \mathbb{R}^{I_n}$ is denoted $\boldsymbol{\mathcal{X}} \times_n \mathbf{u}$ and has entries $(\boldsymbol{\mathcal{X}} \times_n \mathbf{u})_{i_1 \ldots i_{n-1} i_{n+1} \ldots i_N} = \sum_{i_n=1}^{I_n} x_{i_1 i_2 \ldots i_N} u_{i_n}$.

A.3.1 MxD weight tensors through the Khatri-Rao product

MxDs construct the collective weight tensor through the Khatri-Rao product $\odot$ [34] of the two factor matrices $\mathbf{C} \in \mathbb{R}^{N \times O}$, $\mathbf{D} \in \mathbb{R}^{H \times O}$. Concretely, the mode-3 unfolding[3] of the third-order weight tensor $\boldsymbol{\mathcal{W}} \in \mathbb{R}^{N \times H \times O}$ in MxDs from Equation (4) is alternatively given by:

$$\mathbf{W}_{(3)} := (\mathbf{C} \odot \mathbf{D})^{\top} \in \mathbb{R}^{O \times (N \cdot H)}. \tag{15}$$

Given that the factor matrices are learned end-to-end without constraints, they are likely of full column-rank, i.e. $\text{rank}(\mathbf{D}) = \text{rank}(\mathbf{C}) = O$ (as $N > O$, $H = 4 \cdot O > O$ in practice given the MLP layers' larger bottleneck). Consequently, their Khatri-Rao product parameterizing the collective N experts' weights will be of maximum rank O too, through Lemma 1 of [91]. As a result, parameterized this way, the O-dimensional fibers likely span the full output space.

A.3.2 Tensorized MxD forward pass

Furthermore, the layer's forward pass can then be viewed as performing two tensor contractions between the third-order weight tensor $\boldsymbol{\mathcal{W}} \in \mathbb{R}^{N \times H \times O}$ (collecting all N experts' $H \times O$-dimensional matrices) and expert coefficients $\mathbf{a} \in \mathbb{R}^{N}$ and hidden activations $\mathbf{z} \in \mathbb{R}^{H}$. This can be expressed in terms of the so-called mode-n product (denoted by $\times_n$) [34] as follows:

$$\begin{aligned} \hat{\mathbf{y}} &= \sum_{n=1}^{N} a_n \cdot \left(\mathbf{W}_n^{\top} \mathbf{z} \right) \\ &= \sum_{n=1}^{N} a_n \sum_{h=1}^{H} \mathbf{w}_{nh} z_h = \sum_{n=1}^{N} \sum_{h=1}^{H} a_n z_h \mathbf{w}_{nh} \\ &= \boldsymbol{\mathcal{W}} \times_1 \mathbf{a} \times_2 \mathbf{z} \in \mathbb{R}^{O}. \end{aligned} \tag{16}$$

A.4 GLU encoders are a mixture of rank-1 linear experts

Both the proposed MxDs and Gated Linear Units (GLUs) [33] share a similar functional form, using the element-wise product. However, there are crucially important differences between GLUs and MxDs that make both their interpretation and model capacity different.

In short, the technical results here in our paper show that GLUs' encoder can be viewed as a linear mixture of expert layer with rank-1 experts. Furthermore, GLUs can be modified and extended to MxDs with two additions to their model form as detailed at the end of this subsection. First, recall that the GLU encoder [33] computes:

$$\mathbf{y}_{\text{GLU}} = \psi(\mathbf{E}_{\text{GLU}}^{\top} \mathbf{x}) * \left(\mathbf{E}^{\top} \mathbf{x} \right) \in \mathbb{R}^{H}, \tag{17}$$

for input vector $\mathbf{x} \in \mathbb{R}^{I}$, learnable weights $\mathbf{E}_{\text{GLU}}$, $\mathbf{E} \in \mathbb{R}^{I \times H}$, and activation function $\psi(.)$. To transform Equation (17) into the same model form as MxDs, we first pre-multiply the LHS by the identity matrix to match the MxD model form of Equation (5), yielding:

$$\mathbf{y}_{\text{GLU}} = \left(\mathbb{I}^{\top} \mathbf{a} \right) * \left(\mathbf{E}^{\top} \mathbf{x} \right), \tag{18}$$

[3] which is simply a reshaping of a higher-order tensor into a matrix, arranging all N expert matrices' column vectors along the columns of a new matrix.

where $\mathbf{a} = \psi(\mathbf{E}_{\text{GLU}}^\top \mathbf{x}) \in \mathbb{R}^H$ and $\mathbb{I} \in \mathbb{R}^{H \times H}$ is the H-dimensional identity matrix. Next, we can write this explicitly in terms of a linear MoE with expert weights $\mathbf{W}_n \in \mathbb{R}^{I \times H}$ as follows:

$$\mathbf{y}_{\text{GLU}} = \left(\mathbb{I}^\top \mathbf{a}\right) * \left(\mathbf{E}^\top \mathbf{x}\right) \tag{19}$$

$$= \sum_{n=1}^{H} a_n \left(\mathbf{W}_n^\top \mathbf{x}\right) \tag{20}$$

$$= \sum_{n=1}^{H} a_n \left(\mathbf{E}\,\text{diag}\left((\mathbb{I})_n\right)\right)^\top \mathbf{x}\Big), \tag{21}$$

where $(\mathbb{I})_n \in \mathbb{R}^H$ is the n^{th} row of the H-dimensional identity matrix (i.e. a one-hot vector with its only non-zero element at index n). We draw particular attention to how the n^{th} expert's matrix $\mathbf{W}_n = \mathbf{E}\,\text{diag}\left((\mathbb{I})_n\right) \in \mathbb{R}^{I \times H}$ essentially picks out the n^{th} column of $\mathbf{E}$, leaving all remaining $H-1$ columns as zero vectors. **Therefore, GLU encoders compute a MoE with linear expert weights of (at most) rank 1**. This relationship between GLUs and conditional computation is consistent with prior work interpreting individual GLU column vectors as experts [92]. Whilst GLUs' encoders' model form does not put any inherent restrictions on the total number of rank-1 terms that can contribute to the output, the sparsity necessary for specialization does.

We conclude this section by summarizing the two technical changes needed to transform GLUs into full-rank linear MoEs based on the Hadamard product:

1. Replace $\mathbb{I}$ in Equation (18) with learnable, non-diagonal weight matrices for full-rankness.
2. Choose $\psi(.)$ to produce non-negative, sparse coefficients to encourage specialization through sparsity among the experts (for example, a `softmax` function, or a `ReLU` activation followed by `TopK`).

The first of the steps above provides full-rankness, whilst the second brings the sparsity and non-negativity needed for specialization. We include a notebook showing this connection in PyTorch at: https://github.com/james-oldfield/MxD/blob/main/glus-to-moes.ipynb.

A.5 Hadamard-factorized tensors generalize MoVs

Prior work [37] proposes to linearly combine N many $(\texttt{IA})^3$ adapters [38] for parameter-efficient MoEs for instruction fine-tuning. The implementation results in a very similar functional form to the factorized forward-pass in MxDs. Interestingly, the Hadamard product parameterization of the third-order weight tensor in Equation (4) provides a more general framework through which one can also derive MoVs' model form, shedding light on the relationship to the proposed MxDs and their benefits. Concretely, factorizing the weight tensor instead along the *second* mode as $\boldsymbol{\mathcal{W}}(n, :, o) = \mathbf{c}_n * \mathbf{d}_o \in \mathbb{R}^H$ in our framework immediately recovers MoV [37] as a special case. In particular, in contrast to the MxD in Appendix A.3 whose weight tensor can be parametrized equivalently through its mode-3 unfolding [34], MoV's implicit weight tensor can be given in terms of its mode-2 unfolding in terms of a similar Khatri-Rao product of two factor matrices.

Instead, MoVs in analogy would yield expert weights by pre-multiplying $\mathbf{D}$ as: $\mathbf{W}_n = \text{diag}(\mathbf{c}_n)\,\mathbf{D} \in \mathbb{R}^{H \times O}$ for much larger $\mathbf{C} \in \mathbb{R}^{N \times H}$). Due to $H \gg O$, **our proposed MxD formulation yields around $4\times$ the number of specialized units as MoVs** with the same parameter budget (yet MoVs' experts are of no higher rank than MxDs'), making MxDs a much more suitable and efficient class of layer for our goal of scalable specialization. We therefore see that the proposed lens of tensor methods for unification provides valuable insights about how to design more interpretable layers with the minimum trade-off to capabilities.

B Additional quantitative results and ablations

B.1 Faithfulness in output space

Our main experiments measure model faithfulness in latent space–how well the sparse layer variants reconstruct the intermediate MLPs' mapping. Here, we provide additional experiments comparing the faithfulness of sparse layers as their computation propagates to the model output space. Concretely,

we sample 32 consecutive tokens with the base model and then measure how similar the same generations are when the target MLP layer is replaced with the sparse layers.

We sample 512 text snippets from OpenWebText, and use the first 4 words of each as the initial prompts, generating 32 future tokens after each prompt. We plot in Figures 6 and 7 the percentage of the samples' continuations that are identical in the original LLM and hooked LLMs up to n future tokens ahead. We note that this is a rather punishing task–any small deviations quickly compound as n grows. Despite this, we see that the MxDs match the future token generations far better than the baselines, exhibiting more faithfulness in model output space (as well as in latent space).

We also show qualitative examples of the first 8 prompts and the subsequent 'diffs' (using Python 3's `difflib`) of the generated tokens in Figures 8 and 9, where MxDs' superior preservation can be viewed qualitatively.

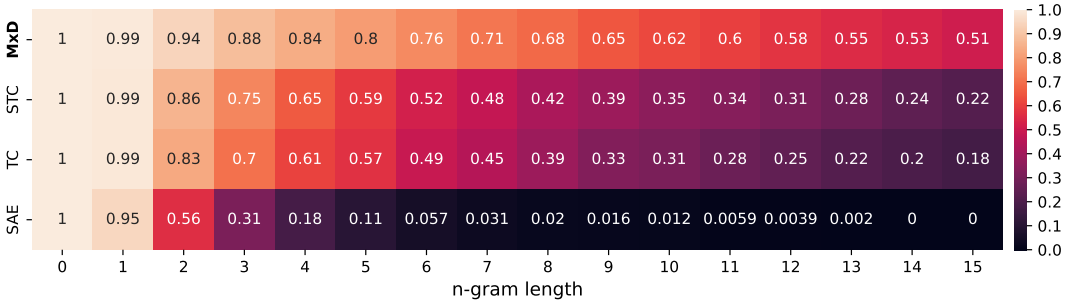

Figure 6: **Pythia-410m**: The percentage of 512 generated samples that contain n words identical to the original model's output (when replacing the base LLM's MLP layer with the sparse layers).

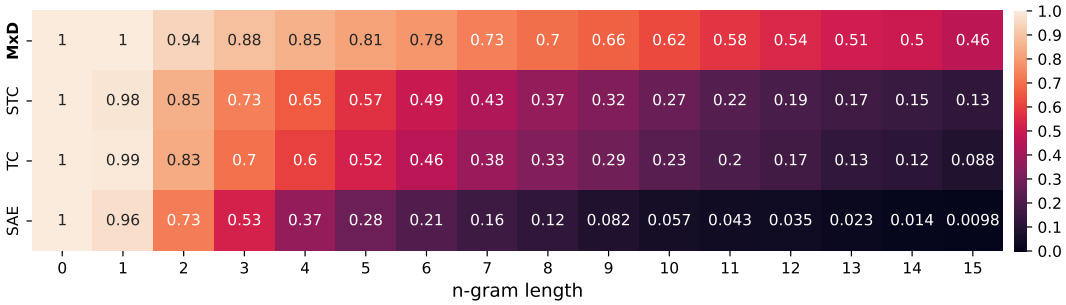

Figure 7: **GPT2-124m**: The percentage of 512 generated samples that contain n words identical to the original model's output (when replacing the base LLM's MLP layer with the sparse layers).

B.2 Additional reconstruction metrics

To highlight the scale of difference in the reconstructions between MxDs and the baselines, we also plot in Figure 10 the normalized MSE at the end of training for all models and LLMs. At the smallest values of K (which we care about most for interpretability), **MxDs' normalized MSE is up to an order of magnitude smaller than Transcoders'**.

B.3 Results on additional layers

We also fully train all models and baselines (with 4 different values of K) on different target layers for each model. The results are shown in Figure 11 for 48 additional trained layers for the same setup in the original paper, using different colours to highlight that these are new results. As can be seen, the same trend holds: MxDs significantly outperform the baselines at small K in all LLMs.

Generation 1, Pythia-410m

GT: **There are times when you need to take a break from your daily routine and just**
MxD: There are times when you need to take a break from your daily routine and just
STC: There are times when you need to be able to do something that is not easy.
TC: There are times when you need to take a break from your daily routine and just
SAE: There are times when you need to be in the air, but not in a high-speed

Generation 2, Pythia-410m

GT: **Humanitarian chief warns capacity of US to be tested By Staff reports Published: Friday, May 30,**
MxD: Humanitarian chief warns capacity of US to be tested By Staff reports Published: Friday, May 30,
STC: Humanitarian chief warns capacity of US to be tested By Associated Press Published: Tuesday, March 29,
TC: Humanitarian chief warns capacity of US to be tested By Associated Press | January 24, 2013
SAE: Humanitarian chief warns capacity of the U.S. military to be a threat The U.S. military is

Generation 3, Pythia-410m

GT: **During the Trump administration, the Department of Homeland Security has been tasked with overseeing immigration enforcement.**
MxD: During the Trump administration, the Department of Homeland Security (DHS) has been tasked with protecting Americans
STC: During the Trump administration, the Department of Justice has been accused of using “bribery” to influence
TC: During the Trump administration, the Department of Homeland Security has been tasked with overseeing immigration enforcement.
SAE: During the Trump administration, the president-elect’s campaign was a “crisis” that could be solved by a

Generation 4, Pythia-410m

GT: **Romanian newspaper ZF.ro cites a report from the Ministry of Interior and Security (MIS) that shows**
MxD: Romanian newspaper ZF.ro cites a report from the Ministry of Interior and Security (MIS) that shows
STC: Romanian newspaper ZF.ro cites a report by the European Commission that shows that Romania is not
TC: Romanian newspaper ZF.ro cites a report from the Ministry of Foreign Affairs and Trade (MFA) that
SAE: Romanian newspaper ZF.ro cites a report that the country's police officers are not allowed to use

Generation 5, Pythia-410m

GT: **Democratic Virginia Gov. Terry McAuliffe (D) on Tuesday said he will not seek re-election in 2020,**
MxD: Democratic Virginia Gov. Terry McAuliffe (D) on Tuesday said he will not seek re-election in 2020,
STC: Democratic Virginia Gov. Terry McAuliffe (D) is running for president in the 2020 election, but he’s
TC: Democratic Virginia Gov. Terry McAuliffe (D) is facing a challenge from a group of Democratic state
SAE: Democratic Virginia Gov. Terry McA. Gingis is a Democrat, but he's not the most popular governor

Generation 6, Pythia-410m

GT: **A federal court has ruled that the Trump administration’s travel ban on people from seven Muslim-majority**
MxD: A federal court has ruled that the Trump administration’s travel ban on people from seven Muslim-majority
STC: A federal court has ruled that the Trump administration’s travel ban on people from seven Muslim-majority
TC: A federal court has ruled that the Trump administration’s travel ban on people from seven Muslim-majority
SAE: A federal court has ordered a former U.S. ambassador to the United Nations, William H. Taylor,

Generation 7, Pythia-410m

GT: **British Columbia takes in \$1.5 billion from the sale of its oil and gas reserves The**
MxD: British Columbia takes in \$1.5 billion from the sale of its oil and gas reserves The
STC: British Columbia takes in \$1.5 billion in tax breaks The British Columbia government has announced that
TC: British Columbia takes in the world The British Columbia government has announced that it will spend
SAE: British Columbia takes in the third year of a plan to expand its coal-mining operations, but

Generation 8, Pythia-410m

GT: **Earlier this month, I wrote about the upcoming release of the first episode of The Walking**
MxD: Earlier this month, I wrote about the upcoming release of the first episode of The Walking
STC: Earlier this month, I wrote about the upcoming release of the “Sonic Boom” soundtrack. The album
TC: Earlier this month, I wrote about the upcoming release of the “Sonic Mania” game. The game
SAE: Earlier this month, I was invited to a conference in the city of Toronto. The event

Figure 8: **Pythia-410m**: The first few generated tokens from the base model (‘**GT**’) and the corresponding tokens from the model when the sparse layers replace the target MLP. Red denotes tokens that are removed, orange denotes newly inserted tokens, and green denotes matching tokens.

B.4 Expert rank

This section concerns the matrix rank of the linear experts in parameter-efficient MoEs. We first compare to low-rank MoEs in Appendix B.4.1 to demonstrate the benefits of full-rankness, and then follow up in Appendix B.4.2 by confirming that the learned MxD expert ranks are close to maximum in the trained models.

B.4.1 Comparisons to low-rank MoEs

In this section, we study the impact of expert rank on the ability of efficient MoE layers to reconstruct pre-trained MLP layers’ mappings. One compelling alternative to MxDs for efficient conditional computation is the μMoE layer [40], which imposes low-rankness on expert weights to achieve parameter-efficiency. Whilst μMoEs are found to perform competitively in the pre-training setting, the impact of low-rankness on approximations of *existing* layers will determine their suitability in the sparse layer approximation setting studied in this work.

Generation 1, GPT2-124m

GT: **There are times when you need to be a little more careful with your food. You**
MxD: There are times when you need to be on the lookout for a new job. But,
STC: There are times when you need to get out of bed and go to the bathroom.
TC: There are times when I feel like I'm being judged. I've been told that my grades
SAE: There are times when you need to get a little bit more than your usual. You're

Generation 2, GPT2-124m

GT: **Humanitarian chief warns capacity to handle refugees is 'unprecedented' The UN refugee agency has warned that**
MxD: Humanitarian chief warns capacity to handle refugees 'is at risk' The UN refugee agency has warned
STC: Humanitarian chief warns capacity to handle emergencies is at risk The UK government has warned that
TC: Humanitarian chief warns capacity to handle emergencies is at risk The UK government has warned that
SAE: Humanitarian chief warns capacity to hold up The BBC's political correspondent, Peter Robinson, says the government

Generation 3, GPT2-124m

GT: **During the Trump administration, the White House has been working to make sure that its immigration**
MxD: During the Trump administration, the White House has been working to make sure that its immigration
STC: During the Trump administration, the White House has been working to make sure that it is
TC: During the Trump administration, the White House has been working to make sure that no one
SAE: During the Trump administration, the White House has been working on a plan to build a

Generation 4, GPT2-124m

GT: **Romanian newspaper ZF.ro cites a report by the European Commission that the country's government is considering**
MxD: Romanian newspaper ZF.ro cites a report by the European Commission that the country's government is considering
STC: Romanian newspaper ZF.ro cites a report by the European Commission that the country's government is considering
TC: Romanian newspaper ZF.ro cites a report by the European Commission that the EU is considering imposing
SAE: Romanian newspaper ZF.ro cites the "revelation" of the "death of the country's economy" as a key

Generation 5, GPT2-124m

GT: **Democratic Virginia Gov. Terry McAuliffe (D) said he would not seek re-election in 2018, but he**
MxD: Democratic Virginia Gov. Terry McAuliffe (D) said he would not seek re-election in 2018, but he
STC: Democratic Virginia Gov. Terry McAuliffe (D) has said he will not support a bill that would
TC: Democratic Virginia Gov. Terry McAuliffe (R) has said he will not seek re-election in 2018, but
SAE: Democratic Virginia Gov. Terry McAuliffe (R) has signed a bill that would allow the state to

Generation 6, GPT2-124m

GT: **A federal court has ordered the Department of Justice to pay \$1.5 million to a group**
MxD: A federal court has ordered the Department of Justice to pay \$1.5 million to a group
STC: A federal court has ordered the Department of Justice to stop using a search warrant to
TC: A federal court has ordered the Department of Justice to stop using a search warrant to
SAE: A federal court has ordered the Department of Justice to pay \$1.5 million to a former

Generation 7, GPT2-124m

GT: **British Columbia takes in \$1.5 billion annually from the federal government, but only about half of**
MxD: British Columbia takes in \$1.5 billion in foreign aid annually, according to the government's latest report
STC: British Columbia takes in \$1.5 billion in foreign aid annually, according to the Canadian Council of
TC: British Columbia takes in \$1.5 billion annually from the federal government, but it's not a big
SAE: British Columbia takes in \$1.5 million in revenue from the province's tourism industry, according to a

Generation 8, GPT2-124m

GT: **Earlier this month, I wrote about the state of our industry. We've been in a bit**
MxD: Earlier this month, I wrote about the state of our industry. We've been in a state
STC: Earlier this month, I wrote about the state of the art in building a solid foundation
TC: Earlier this month, I wrote about the state of the art for creating a custom 3D
SAE: Earlier this month, I was asked to write a piece about the "anti-Semitic" movement in Germany.

Figure 9: **GPT2-124m**: The first few generated tokens from the base model ('**GT**') and the corresponding tokens from the model when the sparse layers replace the target MLP. Red denotes tokens that are removed, orange denotes newly inserted tokens, and green denotes matching tokens.

We therefore compare to μMoE layers, which we use to compute a linear MoE in place of the MLP's decoder. In CPμMoEs, N experts' weight matrices are jointly parameterized through low-rank tensor structure with the CP decomposition [93, 94] for chosen rank $R \in \mathbb{N}^+$. With the same learnable encoder and expert gating matrices producing the expert coefficients $\mathbf{a} \in \mathbb{R}^N$ and hidden units $\mathbf{z} \in \mathbb{R}^H$ generated the same way as in the main paper, we train μMoE layers to approximate the original MLP layer's output with:

$$\mu\text{MoE}(\mathbf{x}) = \sum_{n=1}^{N} \sum_{h=1}^{H} \sum_{r=1}^{R} a_n z_h \, \mathbf{D}(r,h) \cdot \mathbf{C}(r,n) \cdot \mathbf{W}(:,r) \in \mathbb{R}^O, \tag{22}$$

where $\mathbf{C} \in \mathbb{R}^{R \times N}$, $\mathbf{D} \in \mathbb{R}^{R \times H}$, $\mathbf{W} \in \mathbb{R}^{O \times R}$ are the learnable low-rank terms of the implicit third-order tensor parameterizing all N collective experts' weights.

We match the MxD experimental configuration as closely as possible for a fair comparison. For the encoders, we mirror MxDs and use the `GELU` activation function, which we find through ablations in Appendix B.6 to perform the best. We initialize the parameters the same as MxDs and Skip

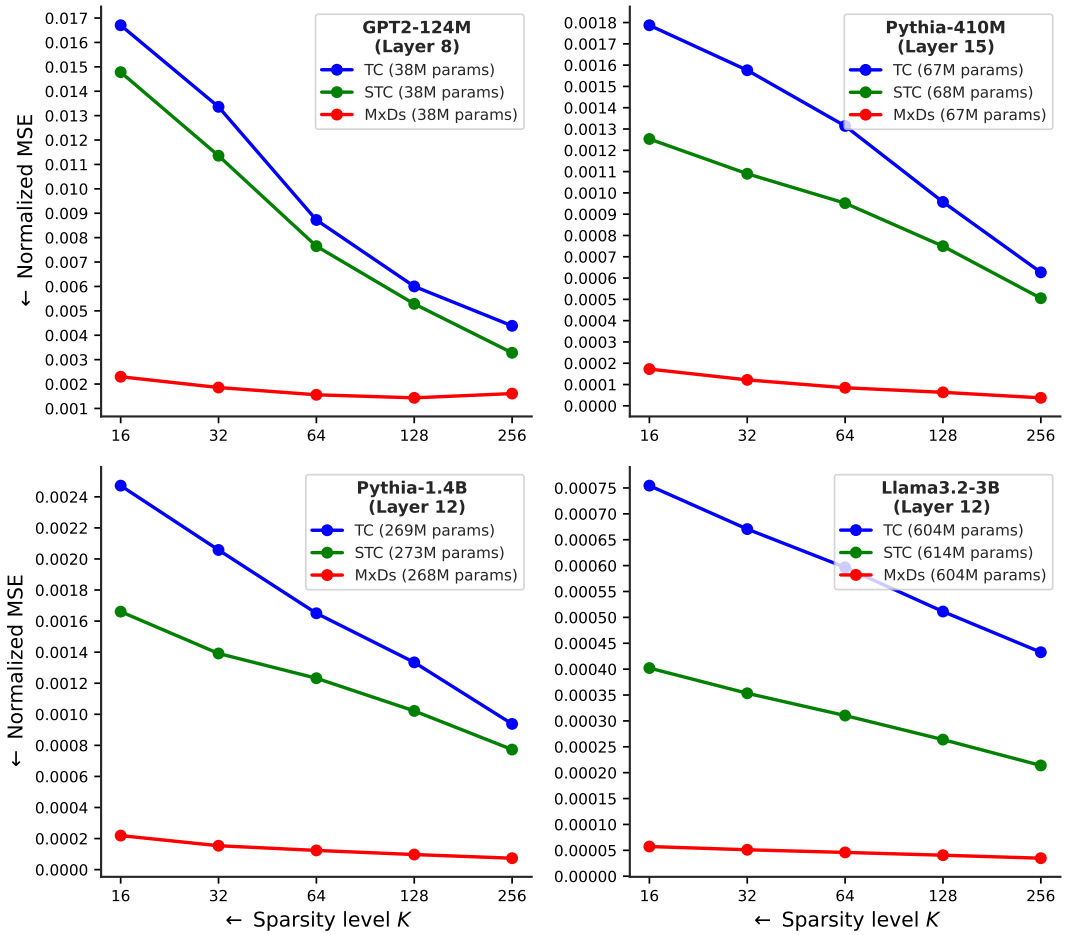

Figure 10: **Normalized MSE** at the end of training Sparse MLP layers, as a function of the number of active units (i.e., hidden neurons vs experts); with differences as large as an order of magnitude in error.

Transcoders: we use the standard PyTorch linear layer initialization for $\mathbf{D}$, $\mathbf{C}$ (and the encoder layers), and initialize $\mathbf{W}$ as the zero matrix.

We vary the μMoE layer rank R, training fully 3 sparse approximation layers for $K = 32$ active experts, varying the total number of experts N to keep the parameter count the same–isolating the impact of the choice of rank. As with the main experiments, we record the downstream model loss when we splice in the trained layer to replace the MLP layers, shown in Figure 12.

As can be seen, the μMoE layers perform well when they are close to full-rank (i.e. when the normalized rank $\frac{R}{O} \to 1$). Crucially, however, performance drops off notably when the rank is reduced. Whilst μMoEs still perform far better than neuron-level sparsity methods (i.e. the corresponding CE loss results in Figure 3), we observe that full-rankness is necessary for the most faithful layer approximations–which the proposed MxDs provide by design.

As a motivating example, for why SparseMoEs and SoftMoEs are not practical: SparseMoEs [36] and SoftMoEs [70] require 2.16 **trillion** parameters for a single layer, for the same 86k experts we use for `Llama-3.2-3B`. This is orders of magnitude more parameters than the entire base network itself, making it prohibitively costly for SparseMoEs to scale to sufficiently high expert counts.

B.4.2 MxD empirical expert rank

Next, we show experimentally that the learned experts' matrices $\mathbf{W}_n = \mathbf{D}\,\mathrm{diag}(\mathbf{c}_n) \in \mathbb{R}^{H \times O}$ are very nearly full-rank in practice, corroborating the properties of expert matrices shown theoretically

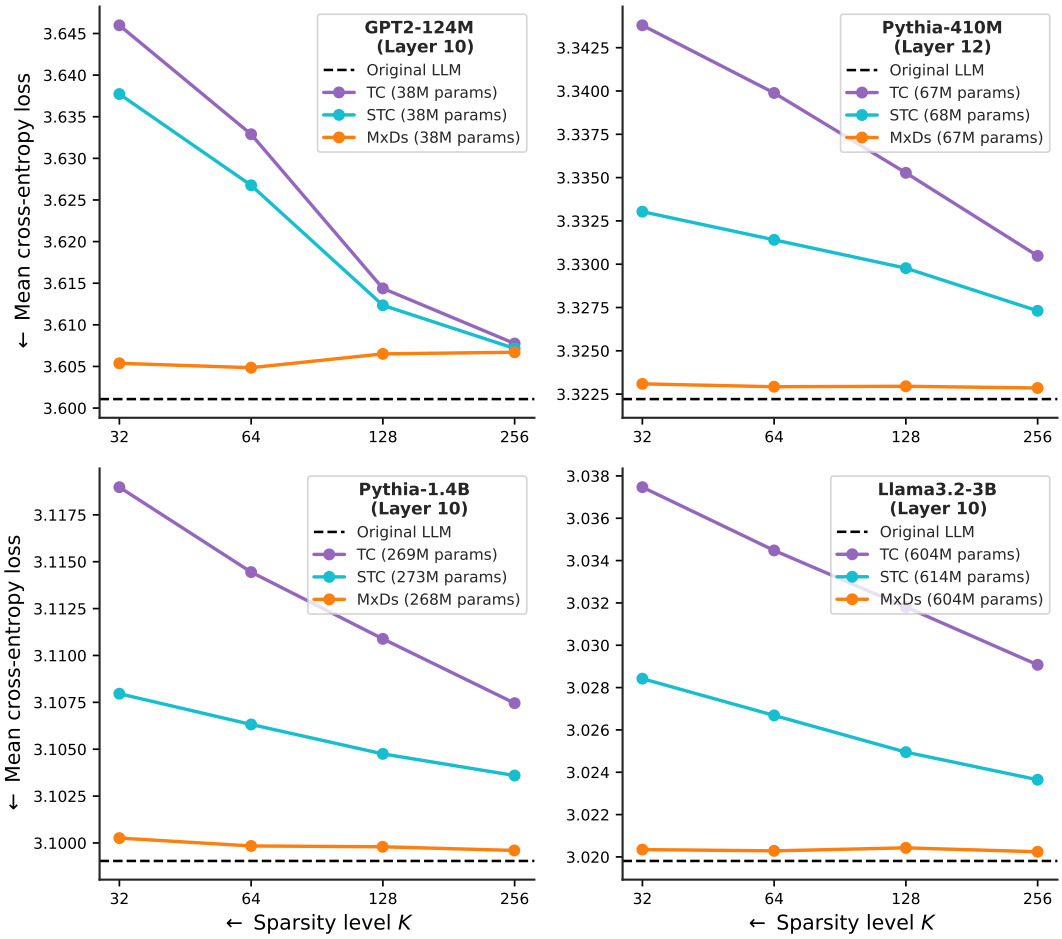

Figure 11: **Additional layer results**: model cross entropy loss preserved when replacing MLPs with Transcoders [27], Skip Transcoders [26], and MxDs, as a function of the number of active units (hidden neurons/experts). These results complement those in the main paper, but here we train a new set of additional models on different layers.

in Lemma 1. We compute the mean 'normalized rank', which we take for MxDs to be the empirical matrix rank of the learned expert's weights, over the maximum possible rank given the dimensions:

$$\frac{1}{N}\sum_{n=1}^{N}\frac{\text{rank}\left(\mathbf{W}_n\right)}{\min\{H,O\}}. \tag{23}$$

We show in Table 3 the normalized rank across all 4 base models: MxD's learned experts exhibit no rank deficiencies, providing further evidence of the large potential capacity of MxD layers despite their sparsity constraints on the expert-level.

Table 3: Mean normalized expert matrix rank of Equation (23) across models for the first 2k experts in $K = 32$ trained MxDs – the learned expert matrices are very close to full column rank.

GPT2-124M	Pythia-410M	Pythia-1.4B	Llama-3.2-3B
0.99 ± 0.005	0.99 ± 0.007	0.99 ± 0.005	0.99 ± 0.002

B.5 Sparse probing

Sample-level probing Here, we follow the SAEBench [19] evaluation protocol. In this 'sample-level' setting, each text string is labeled with a binary concept at a global level (e.g., the language of

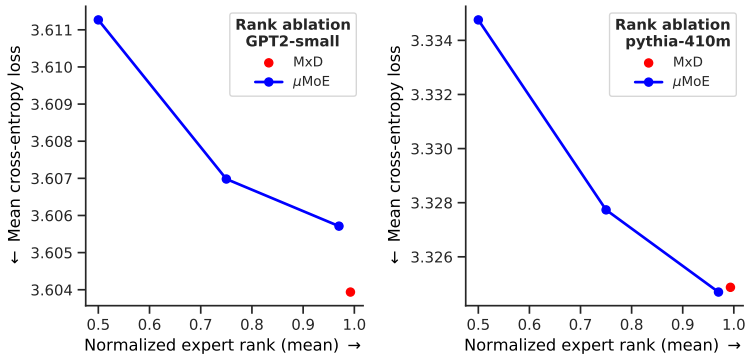

Figure 12: Comparisons to μMoEs for various choices of (normalized) rank: high rank weights best-preserve the models' downstream cross-entropy loss.

Table 4: Details of sample-level sparse probing datasets used.

Dataset	# Training examples	# Test examples	Classification task description	Number of classes
fancyzhx/ag_news [48]	16,000	4,000	News article topic	4
codeparrot/github-code [95]	20,000	5,000	Programming language	5
amazon_reviews_mcauley_1and5_sentiment [96]	8,000	2,000	Positive/negative review sentiment	2
Helsinki-NLP/europarl [97]	20,000	5,000	European language	5
LabHC/bias_in_bios [98]	32,000	8,000	Profession from bio	8

the snippet, or its sentiment). This is in contrast to what we refer to as 'token-level probing', where *each token* within the text samples is labeled individually (e.g., whether a word is a certain part of speech). We perform experiments on a total of 24 sample-level sparse probing tasks with the same 'maximum mean difference' feature filtering applied in [19]. The details of the datasets used are summarized in Table 4.

Token-level probing We also explore sparse probing for 10 features defined at the token-level. For this, we follow [49], and include experiments training probes on the mean feature activations under tokens spanning the **surnames** of the individuals. We note that this is a significantly harder task, and makes even stronger assumptions about the features the dataset includes, but is nonetheless some additional weak evidence about the relative feature-learning abilities of the sparse models. Through various surnames, we probe for 6 occupations of individuals, whether or not individuals are alive, and individuals' labeled gender. We also experimented with probing for compound words as in [49], but found no predictive features in our trained models. Details of the surname token-level probing datasets (and the total training examples the tokenizers could parse) are included in Table 5.

Table 5: Details of token-level sparse probing datasets used.

Dataset	# Training examples	# Test examples	Classification task description	Number of classes
Occupation [49]	4784	1195	Occupation of individual	6
Is alive? [49]	4800	1199	Are they alive	2
Gender [49]	4800	1200	Labeled gender	2

Experimental setup For sample-level probing, we truncate the input strings to the first 128 tokens for all datasets but for the `Github` dataset, where we take the last 128 tokens to avoid license headers [19, 49]. For token-level probing, we instead take only the last 128 tokens, where the final token contains the surname of the individual in question in the datasets of [49].

Binary probes are trained on 80% of the training data (randomly shuffled) with the `sklearn` library's `LogisiticRegression` module with parameters:

- class_weight='balanced'
- penalty='l2'
- solver='newton-cholesky'

- max_iter=200

A random seed of 42 is used throughout the code to ensure reproducibility.

B.5.1 Sparse probing results

We show in Figure 13 results on 20 additional (sample-level) sparse probing tasks, where MxDs remain competitive with the baselines. We also plot the expert activation (of the single expert with the highest F1 test set score) for the positive/negative classes for all tasks split across Figures 14 and 15. One can observe a certain degree of separability between the two semantic clusters of data given by the expert coefficient, thus confirming that individual experts are learning to specialize to particular high-level features.

We also include results on 10 token-level probing tasks in Figure 16, with the corresponding activation densities displayed in Figure 17. Whilst MxDs appear to perform slightly less well here on average, they remain competitive as expected.

B.6 Ablations

We turn next to ablation studies to explore the value of the various model components below:

B.6.1 Choice of sparsity constraint

We first train a variety of MxDs on GPT2 models with the TopK activation function [23] and instead train models with a ReLU followed by an explicit $\lambda||.||_1$ sparsity penalty on the specialized components in addition to the reconstruction loss [22]. We show the results in Figure 18, where, similarly to [26], we find the TopK activation to dominate on the sparsity-accuracy frontier–we thus use the TopK activation for all experiments.

B.6.2 Choice of MxD encoder

Secondly, we show in Figure 19 the benefits of MxDs' flexibility in inheriting the original MLP layer's encoder form/activation function. All models here are trained from scratch for the same number of tokens and with the same experimental setup as in Section 3.1, with $K = 32$. In the first 3 left-most subfigures, we see the Normalized MSE is as low as half when using GELU vs the non-native ReLU activation.

We next ablate the impact of inheriting the same encoder as the `Llama-3.2-3B` base model. In the rightmost subfigure of Figure 19, we train MxDs with ReLU-MLP, GELU-MLP, and Swish-GLU encoders. As can be seen, using a GLU with a Swish activation model (matching the base model architecture) yields a Normalized MSE almost an **order of magnitude** smaller than MLPs with GELU/ReLU.

C Feature balance and shared experts

C.1 Expert/feature balance

Following the code of [27, 99], we log how often each unit of specialism/feature is used, over a fixed window of $\sim$ 1M tokens. We show in Figure 20 the feature frequency at the end of training, where we observe that MxDs see a similar healthy balance of experts to the frequency of usage of features in the baselines.

Interestingly, we observe a small peak of experts that fire more frequently in MxDs (e.g., around -2 on the x-axis)–perhaps specializing in common patterns and primitives in natural language.

C.2 Shared experts

We find that, by default, our MxD models naturally learn to use a shared expert, with the remaining experts exhibiting strong specialization in a wide range of themes and linguistic patterns. The use of a shared expert is becoming an increasingly popular design choice, including in the latest Llama 4 models [44]–we therefore allow this pattern to emerge naturally in our base models, further justified

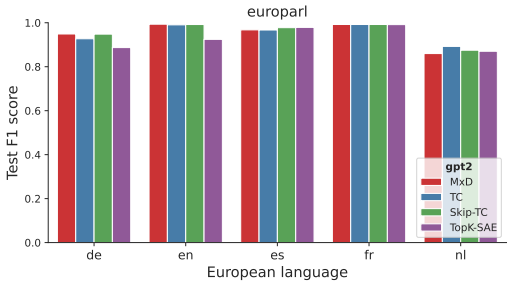

(a) Europarl dataset, on GPT2

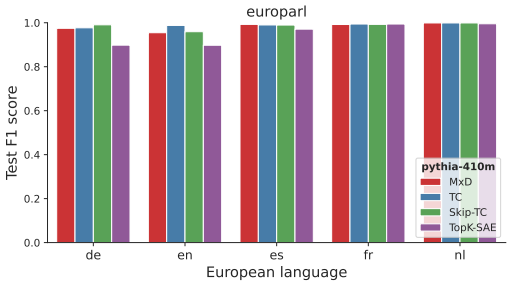

(b) Europarl dataset, on Pythia-410m

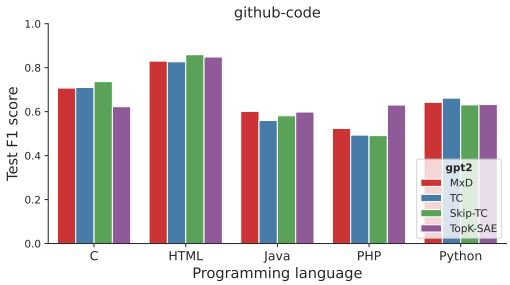

(c) Github code dataset, on GPT2

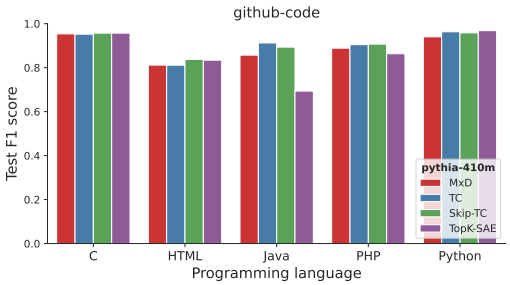

(d) Github code dataset, on Pythia-410m

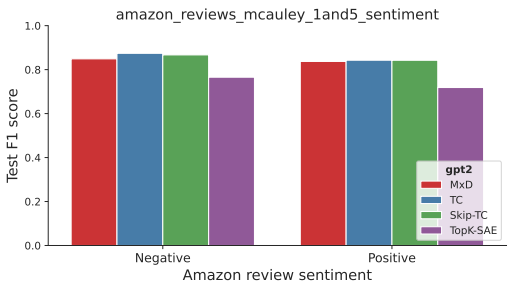

(e) Amazon review sentiment dataset, on GPT2

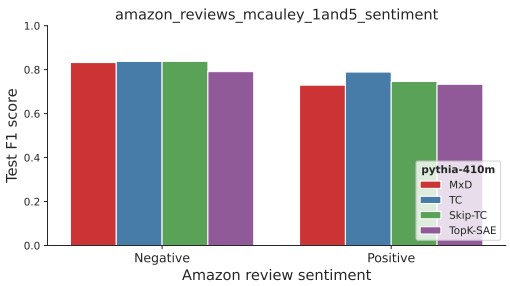

(f) Amazon review sentiment dataset, on Pythia-410m

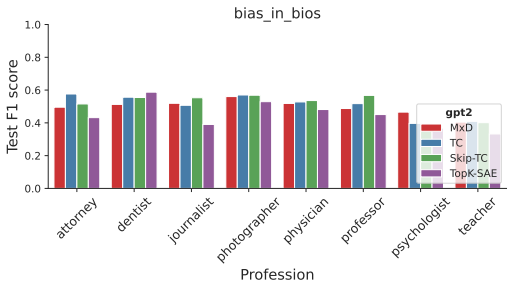

(g) Bias in Bios dataset, on GPT2

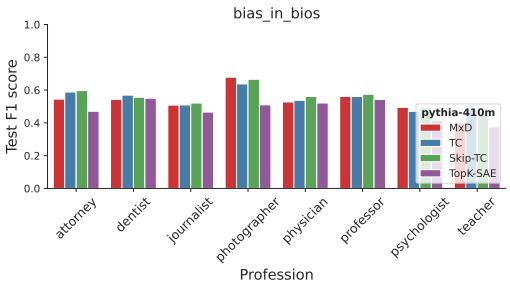

(h) Bias in Bios dataset, on Pythia-410m

Figure 13: **Sample-level** sparse probing results on individual experts/features; the best F1 score on a held out set is presented.

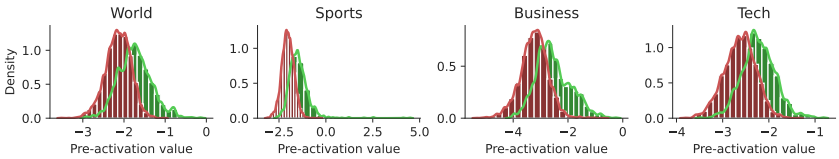

(a) AG news dataset, on GPT2

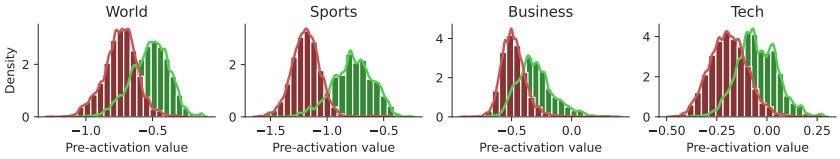

(b) AG news dataset, on Pythia-410m

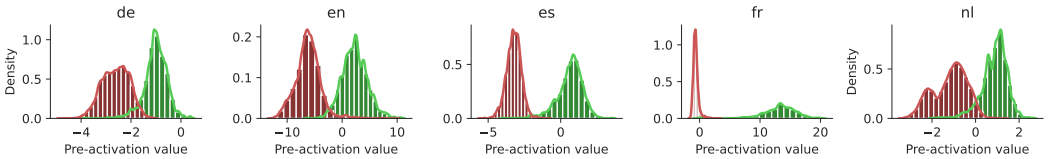

(c) Europarl dataset, on GPT2

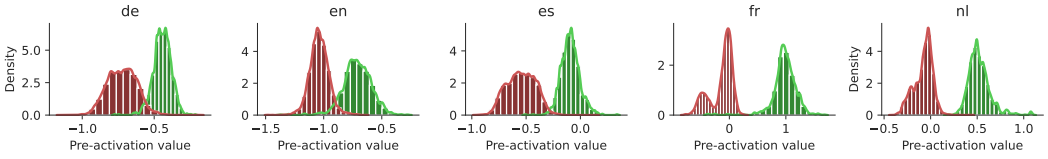

(d) Europarl dataset, on Pythia-410m

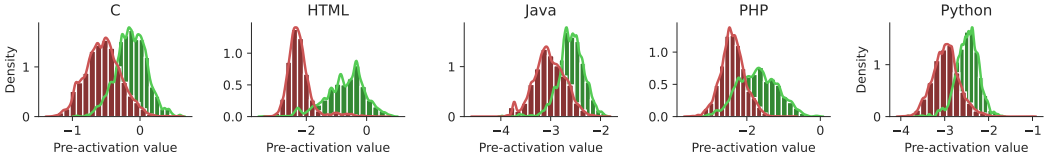

(e) Github code dataset, on GPT2

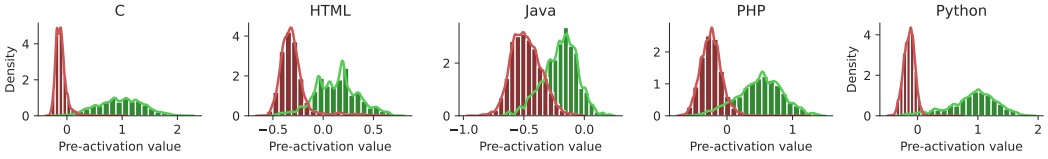

(f) Github code dataset, on Pythia-410m

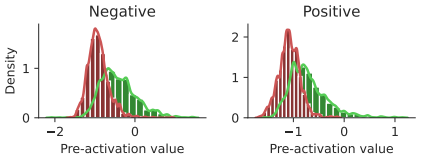

(g) Amazon review sentiment dataset, on GPT2

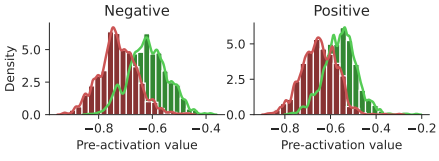

(h) Amazon review sentiment dataset, on Pythia-410m

Figure 14: **[1/2] Sample-level** sparse probing results on individual experts for MxDs; here we plot the values of the expert pre-activation for **positive**/**other** classes (in the 1-vs-all setting).

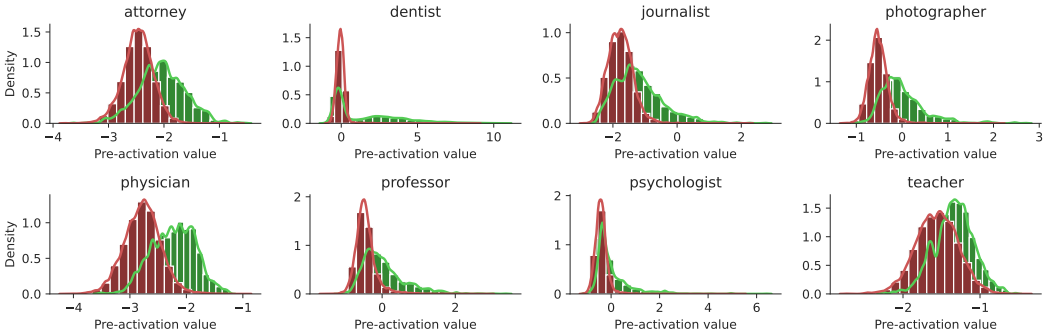

(a) Profession from biography, on GPT2

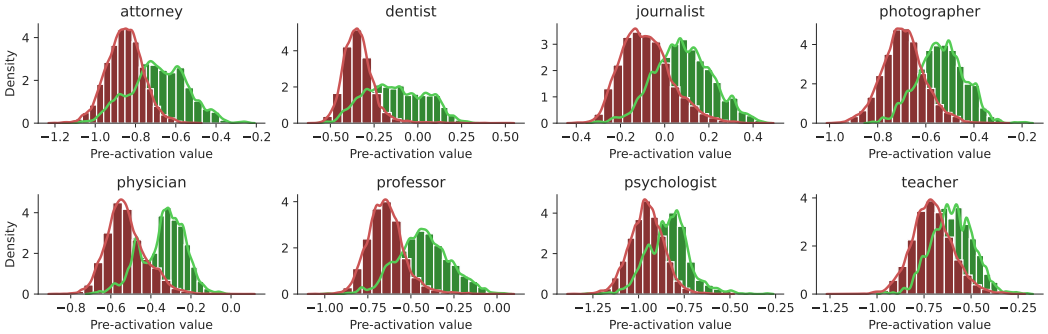

(b) Profession from biography, on Pythia-410m

Figure 15: **[2/2] Sample-level** sparse probing results on individual experts for MxDs; here we plot the values of the expert pre-activation for **positive**/**other** classes (in the 1-vs-all setting).

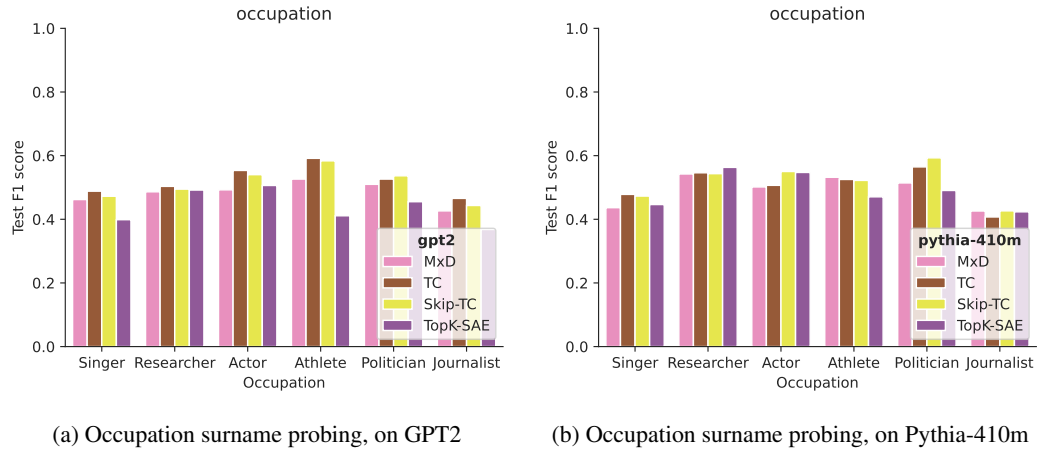

(a) Occupation surname probing, on GPT2

(b) Occupation surname probing, on Pythia-410m

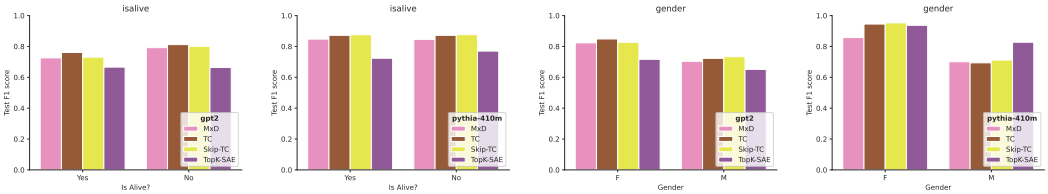

(c) "Is alive?" surname probing, on GPT2

(d) "Is alive?" surname probing, on Pythia-410m

(e) Gender surname probing, on GPT2

(f) Gender surname probing, on Pythia-410m

Figure 16: **Token-level** sparse probing results on individual experts/features; the best F1 score on a held out set is presented.

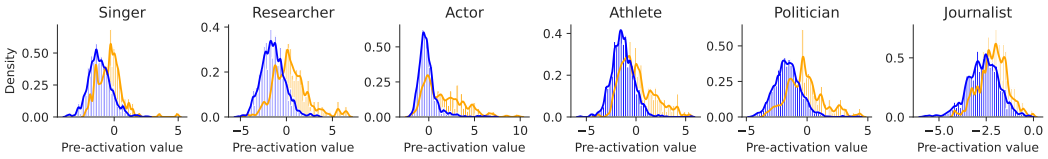

(a) Occupation surname probing, on GPT2

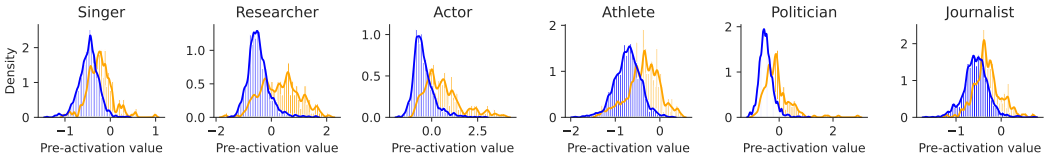

(b) Occupation surname probing, on Pythia-410m

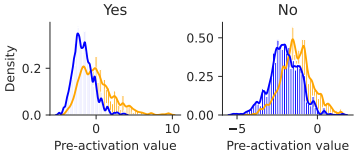

(c) Alive/dead surname probing, on GPT2

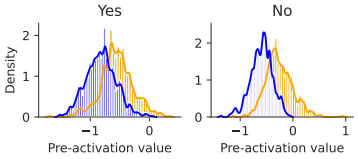

(d) Alive/dead surname probing, on Pythia-410m

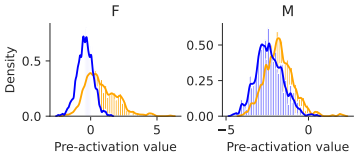

(e) Gender surname probing, on GPT2

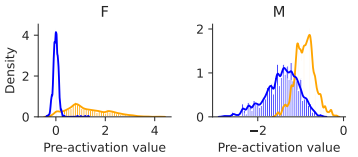

(f) Gender surname probing, on Pythia-410m

Figure 17: **Token-level** sparse probing results on individual experts for MxDs; here we plot the values of the expert pre-activation for **positive**/**other** classes (in the 1-vs-all setting).

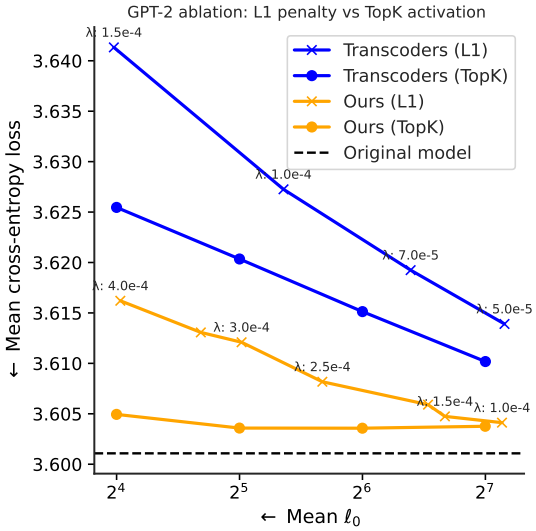

Figure 18: ReLU+TopK activation function [23] vs ReLU w/ L1 sparsity penalty [22]: both MxDs and Transcoders better recover the cross entropy loss with the TopK activation.

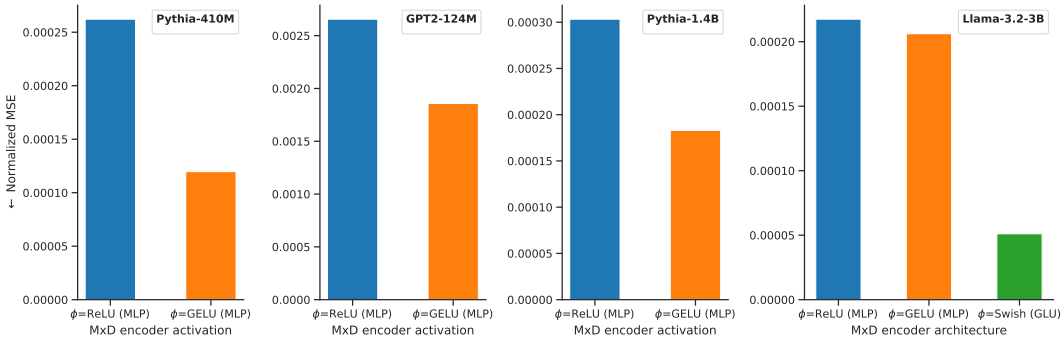

Figure 19: **Encoder architecture ablation**: MSE loss when using ReLU activation vs the GELU used by the base models; and MLPs vs GLUs for Llama (rightmost subfigure).

through the evidence in [43] that shared experts can enhance specialization among the remaining experts [43]. We highlight, however, that a simple trick of sampling $\hat{K} \sim \text{Unif}\{K - K/a, K + K/a\}$ for the Top-$\hat{K}$ activation at train-time (for e.g. $a := 2$) is sufficient to remove the dominating shared-expert at minimal hit to reconstruction performance, if desired.

We train two sets of models with a base $K = 32$ on `GPT2-small` and `pythia-410m`, using $a := 2$. We first show in Figure 21 the indices of the top-activating experts for the 2 model variants on a template prompt, after training has finished. On the left-hand side of Figure 21, the models route all tokens through the same shared expert at position 1. However, we see on the right-hand side that training with the 'random-K' strategy breaks the dependence on a shared expert in position 1. Furthermore, we include in Figure 22 the corresponding train-time MSE loss for the 4 models here as ablations–observing that the random-K strategy also brings comparable performance. Based on these experiments, we recommend this simple training strategy if one desires MxD models without shared experts.

D Detailed experimental setup

We list in Table 6 the resources used for each experiment: the GPU and the indicative run-time for a single model. The `mlp_expansion_factor` column refers to the expansion factor applied to the input dimension to generate the MLP width in the sparse layers (i.e. $H := I \cdot$ mlp_expansion_factor).

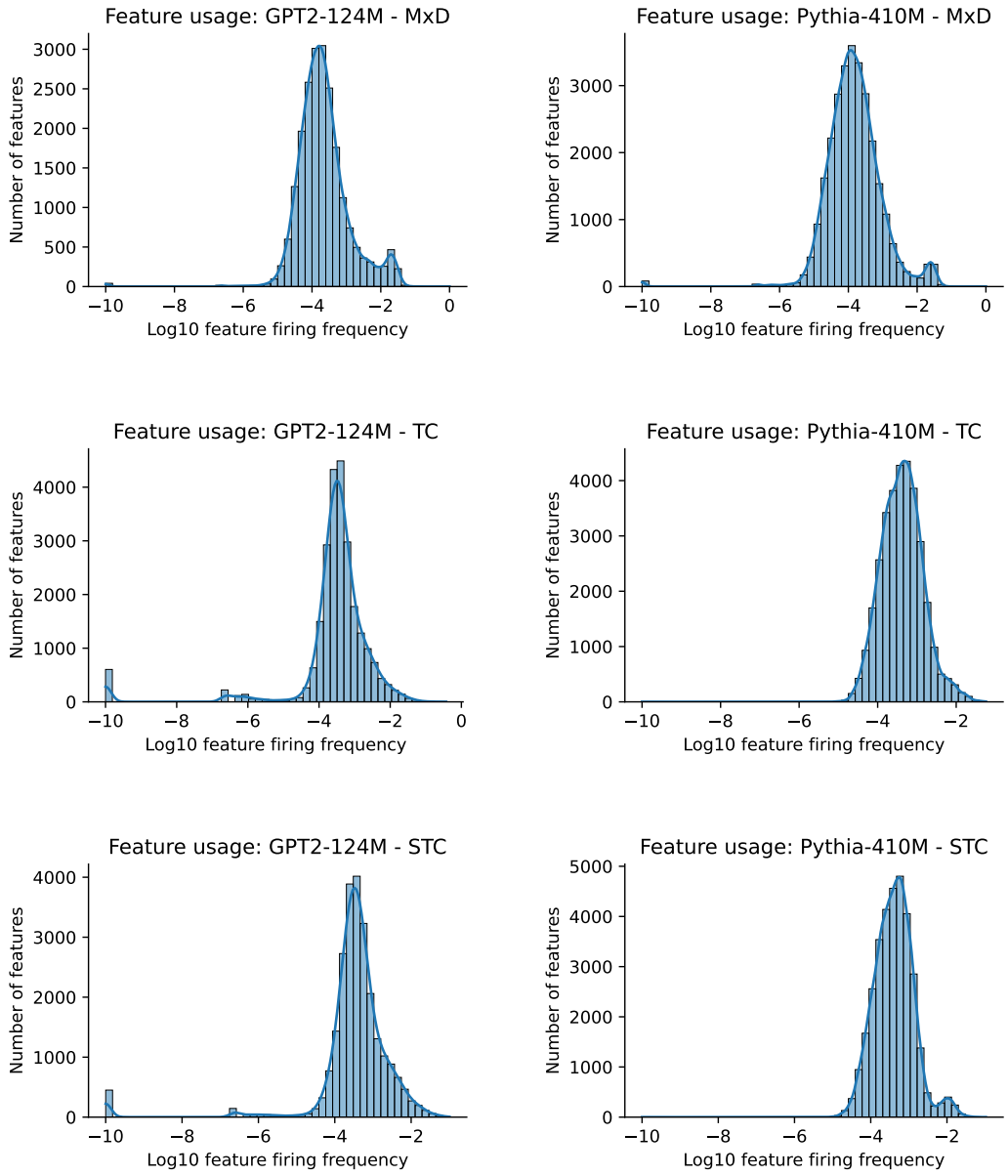

Figure 20: $\log_{10}$ feature sparsity (following [27, 99]); MxDs' experts are well-balanced, similar to the baselines' features.

Table 6: Total training time and resources used to produce the $k = 32$ experiments (the required compute being roughly the same across models trained with different k).

Model	GPU used	VRAM	Training time	d_in	mlp_expansion_factor	Asset link
GPT2-124m	x1 GeForce RTX 3090	24GB	8h 34m 37s	768	32	https://huggingface.co/docs/transformers/en/model_doc/gpt2
Pythia-410m	x1 GeForce RTX 3090	24GB	8h 35m 17s	1024	32	https://huggingface.co/EleutherAI/pythia-410m
Pythia-1.4B	x1 A100	80GB	23h 25m 23s	2048	32	https://huggingface.co/EleutherAI/pythia-1.4b
Llama-3.2-3B	x1 A100	80GB	2d 3m 50s	3072	32	https://huggingface.co/meta-llama/Llama-3.2-3B

Model trained with fixed K

	1st highest expert index	2nd highest expert index	3rd highest expert index	4th highest expert index
Token 1	10160	10962	19772	9610
Token 2	19772	15461	2630	8228
Token 3	19772	18694	7385	3494
Token 4	19772	19466	10619	970

Model trained with **random** K

	1st highest expert index	2nd highest expert index	3rd highest expert index	4th highest expert index
Token 1	526	18499	7257	8244
Token 2	16092	3344	17100	7388
Token 3	19829	10864	7720	5507
Token 4	20001	15277	1905	11387

Prompt: `"Who is the president of the USA?"`

GPT2-small

Model trained with fixed K

	1st highest expert index	2nd highest expert index	3rd highest expert index	4th highest expert index
Token 1	28104	1694	18149	2013
Token 2	28104	1163	5124	11890
Token 3	28104	5124	27687	3657
Token 4	28104	4126	12814	23628

Model trained with **random** K

	1st highest expert index	2nd highest expert index	3rd highest expert index	4th highest expert index
Token 1	7412	13294	3097	19430
Token 2	13439	24209	13723	18099
Token 3	9587	3857	10715	6198
Token 4	2809	3378	25799	9435

Prompt: `"Who is the president of the USA?"`

Pythia-410m

Figure 21: Top-activating experts for template prompt with and without using a randomized value of K at train-time for TopK expert selection: randomization largely prevents a shared expert. Shown are the leading 4 tokens and expert indices.

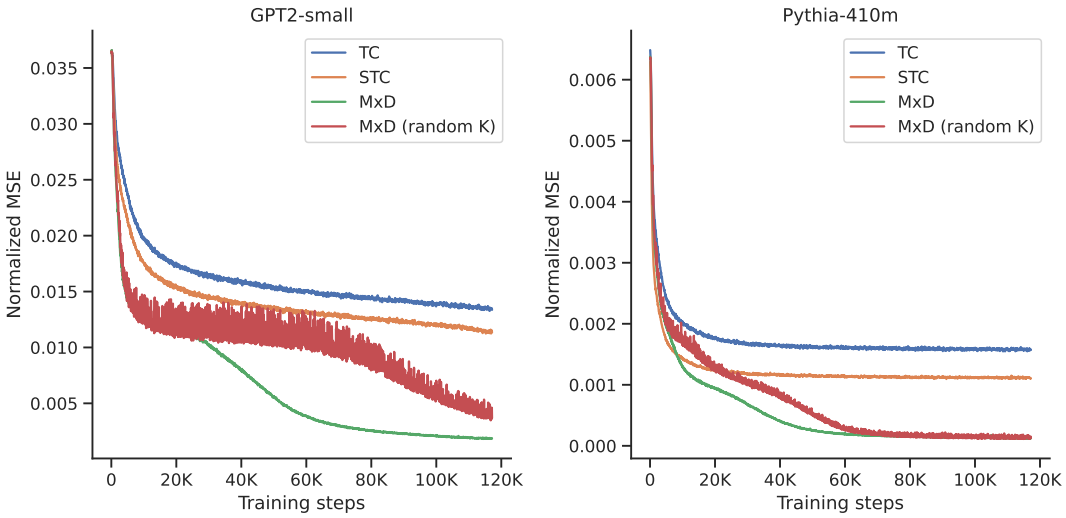

Figure 22: **MxD performance with random K sampling**: Normalized MSE loss as a function of training steps using a fixed Top $K := 32$ expert selection and when sampling $\hat{K} \sim \text{Unif}\left\{K - \frac{K}{2}, K + \frac{K}{2}\right\}$.

D.1 Feature steering details

For the steering experiments, we use two LLM judges to grade generations on two axes. The full template prompt we feed to `gemini-2.0-flash` and `llama-4-scout-17b-16e-instruct` is as follows (note that line breaks and emphases are included here only to aid visualization):

Prompt given to LLM judges

You are an expert evaluator of synthetic text.
TASK: Rate a collection of {num_samples} samples along two independent axes.
AXIS 1 – CONCEPT COHERENCE:
0.00 no shared concepts/themes/style.
0.25 faint overlap.
0.50 some overlap or similar structure.
0.75 mostly the same concepts or structure; a few partial drifts.
1.00 all snippets clearly share the same concepts, themes, style, or structure.
AXIS 2 – GRAMMATICAL FLUENCY:
0.00 incomprehensible.
0.25 dense errors; meaning often obscured.
0.50 frequent errors; meaning still mostly recoverable.
0.75 minor errors that rarely hinder comprehension.
1.00 completely grammatical and natural.
(Do not penalise fluency if a snippet starts or ends abruptly.).
SCORING: Choose any real value in [0, 1] for each axis.
OUTPUT FORMAT: Respond with exactly two numbers formatted '0.00, 0.00' in the order [coherence, fluency] and no other text or symbols.
TEXT TO EVALUATE: {samples}

E Additional qualitative results

We show in Figures 23 and 24 tokens activating the first 9 experts as they appear numerically. We sample 6 bins of expert coefficient value to show both tokens that highly activate the experts and those that do so only mildly. As can be seen, both high- and low-level specializations emerge in both GPT and Pythia models.

Whilst we observe specializations to a range of concepts (such as punctuation, MMO games, words in specific contexts), we do not notice any systemic differences between the types of expert specializations that emerge between the two models in MxD layers.

Pythia-410m: Tokens routed to specific experts

Feature 0

Activation between 3.86 and 4.63
, Vol. 1, No. 1 (2002
Activation between 3.09 and 3.86
, Vol. 1, No. 1 (2002
, Vol. 62, No. 6 (May
of firearms listed below paragraph No 2. It is
Vol. 1, No. 1 (2002
Vol. 25, No. 4 (Oct
NBER Working Paper No. 21611
Activation between 2.32 and 3.09
on Rural Free Delivery Route No. 1, where
Journal Letters 676, No. 1 (20
- Violin Sonata No. 9 in A
- Violin sonata no.1
Activation between 1.54 and 2.32
'Shawn Robinson at No. 10 overall,
Piano Sonata No.1 Op.
agio String quartet no.1 - 3
. Now at No. 5, the
Artist Title String quartet no.1 Brah
Activation between 0.77 and 1.54
Rams in exchange for the No. 15 pick and
Journal of Sociology , Vol. 62, No
th), Canada is ranked no. 10 in the
," International Migration Review, Vol. 27, No
today released ' Report No. 5 of 2016 Init
Activation between 0.00 and 0.77
material Tungsten Premium Nozzles Why
Vol. 1, No. 1 (2002),
Rams in exchange for the No. 2 overall pick
of Shepard as the No. 2 option New
<|endoftext|>rd period, 1

Feature 1

Activation between 3.81 and 4.57
you will. Version 3.20 of
Activation between 3.05 and 3.81
you will. Version 3.20 of
background the installation media runs version 4.4.
to author. Version 1: 15,
, which was introduced in version 3.7.
VERSION is not supported (version 4+ required)"
Activation between 2.28 and 3.05
What's New in Version 2.4
release of RON library version 0.1.
gmail.com> (version=TLS1
It was initially released as version 7.0 on
be issuing some of the version, while Eduard
Activation between 1.52 and 2.28
This was the version that underwent trials on
weakness, affecting the latest version of WordPress, 4
h. It began as version of the Arabic dish
learn more about him at Version One Ventures.
2.10. That version will not necessarily have
Activation between 0.76 and 1.52
have to UNINSTALL this version and RE-INSTALL
fork occurred, creating two versions of Bitcoin: the
by itself with NO other version of the mod installed
developers to bring much newer versions of apps to Ubuntu
the 42 count includes multiple versions of the same song
Activation between 0.00 and 0.76
JS using a slightly modified version of John Resig
? A previous version of this article suggested
Air Force have employed numerous versions of the roundel
somewhat disappointed in the 2015 version as there is not
<|endoftext|>rd period, 1

Feature 2

Activation between 3.01 and 3.61
of release of Starcraft 2, the popularity
Activation between 2.41 and 3.01
of release of Starcraft 2, the popularity
aggered release Although Dota 2 officially launched out
the new generation of Dota players, which inevitably
industry; this gives Dota a more personal feel
going to prefer, Dota 2 is the first
Activation between 1.81 and 2.41
from all the Starcraft 2. The Gr
much additional skill), Dota 2 has become hugely
impossible."A new Overwatch patch is currently in
circuit), the starcraft crowd just exploded in
who had been in Dota casting since the beginning
Activation between 1.20 and 1.81
difficulty of Vanilla WoW because at the end
top teams in Rocket League." - Ted I
active mindset that other MMOs encourage, and
worry about in an MMO, but VoidSpace
As an SC2 fan, I am
Activation between 0.60 and 1.20
Shop items on the MapleStory website. However,
attack. In a MOBA, there's no
, like Dungeons & Dragons or Pathfinder,
you often hear about massively multiplayer online games
like World
in this way. Mass Effect is (mostly)
Activation between 0.00 and 0.60
Wish is a simple exploration RPG, but creates a
the coaching staff of SKT T1 is really
taxis from Morrowind, and the lava
of the stations in the game themselves, be it
<|endoftext|>rd period, 1

Feature 3

Activation between 3.28 and 3.94
Kathmandu, many rescue crews had yet to
Activation between 2.63 and 3.28
Kathmandu, many rescue crews had yet to
severely damaged, hampering rescue and humanitarian
efforts.
while at sea that the rescue had failed. A
, providing minimal protection or rescue work, pulling a
<|endoftext|> his rescue as he was mug
Activation between 1.97 and 2.63
dead, was reported. Recovery was generally slow,
the region to help in rescue operations
box full of tools, recovery equipment and even an
to contribute a "rescue offer", like the
2013 and triggered a massive relief effort. Like Maria
Activation between 1.31 and 1.97
"We immediately began resuscitation procedures, including
medications
was followed by a federal relief effort widely critiqu
in preparation for the hostage rescue mission. Ziem
of damage and amount of recovery time required after the
on relief operation. The rehabilitation process will also
take
Activation between 0.66 and 1.31
damage and began the long cleanup process — an RV
Smoke forces passengers to evacuate plane in Houston
cost-of-service recovery, just as they
as helicopter opens fire Emergency services attend to
injured after
<|endoftext|> comes to the rescue on screen. I
Activation between 0.00 and 0.66
the Atlantic, which made escape for U-Bo
, while DRC is recovering from years of internal
is estimated the cost of repairing the damage could run
challenge is trying to bounce back against the Colorado
Rapids
<|endoftext|>rd period, 1

Feature 4

Activation between 3.09 and 3.71
hole Tournament at 2; Diminishing Jim at
Activation between 2.47 and 3.09
hole Tournament at 2; Diminishing Jim at
St. Joseph Dimensions & Specifications
sci and Marxist Theory, Dimensions of Radical
- M6 Dimanche, le magazine
AM | Konstantinos Dimopoulos / Gnome
Activation between 1.85 and 2.47
V / 60 mA Dimension W6
-ion prismatic Battery, Dimensions 14.16
-car salesmen and dimwitted botox
book Pluralism (Durham: Duke University
Activation between 1.24 and 1.85
that broke, Shaw has dimpled cheeks, a
looked good on a dim cathode ray but not
Take a caster like Durka, for example
American parents of color at Dumbo's P
under-educated families with dim school and life
prospects
Activation between 0.62 and 1.24
Belisol Team 82 Luke Durbridge (Aus
iu cati realizati dimensiunea
failed to note is that Dak Prescott is the
Link I was dumbfounded when I
all 5 Official Main Cast Dakimakura (
Activation between 0.00 and 0.62
outy daughter (Dakota Johnson) catches
L. Vuitton déposée" (
by radical open borders socialist Dolores Huerta-
ers. Airports, Delays,
<|endoftext|>rd period, 1

Feature 5

Activation between 3.51 and 4.21
order » ·Mel Kiper's final
Activation between 2.81 and 3.51
order » ·Mel Kiper's final
<|endoftext|>, Melba 16 19 Mel
like a Saturday night at Mel Gibson's house
Christine Sinclair Melissa Tancred
Basic Books. Melillo, R.,
Activation between 2.11 and 2.81
ir, the producers wanted Melora to have a
Mawson 45 30 Melba 9 Baint
Bashir and Melora are in the
changes his mind and shoots Melora. A charge
in mid-air, Melora tells Bashir
Activation between 1.40 and 2.11
Hitting coach Osmin Melendez told us
charming bedside manner". Melora laughs but,
anging stuff and forget the melodic disco-
us." - Melora and Julian Bash
each other's eyes. Melora suddenly breaks the
Activation between 0.70 and 1.40
Kingsford Smith Drive, Melba 5 22 Mel
10 Linger Place, Melba 10 15 Mel
, Melba 10 19 Melba 15 Crossley
the permafrost melts, a potent
Activation between 0.00 and 0.70
bombs, soak, wax melts what they are
21-year-old Micah David-Cole
B-Type 50MN Microwarpdrive Att
). She was followed by Micheline Calmy
<|endoftext|> points by Mellamphy). He
<|endoftext|>rd period, 1

Feature 6

Activation between 2.57 and 3.09
Keepers is a remarkable and enormously enjoyable
documentary
Activation between 2.06 and 2.57
Keepers is a remarkable and enormously enjoyable
documentary
tackled in a bizarre and post-apocal
dizzying, confusing, and scattering dance-like
, including some very challenging and difficult times in
recent
<|endoftext|> us to this strange and perilous place.
Activation between 1.54 and 2.06
his work such a varied and boundless feel that
titans, a fun and ultra-violent mini
"It is complicated and probably fraught to
reasons for this are complicated and painful but here is
Up the Volume: dangerous and alive and a little
Activation between 1.03 and 1.54
that were the most surprising or impactful.
Hulk is a big and demanding game especially on
, sophisticated, disarming and even counterintuitive
Minister who's rattled and watching Scotland turn its
.Energetic and clean.One of
Activation between 0.51 and 1.03
said something so misguided and distasteful that
s systems are so obscure and complicated that it takes
a quiet, proficient and studious officer.
church, including its complex and sumptuous music
increasingly riven by angry, uncivil rivals with
Activation between 0.00 and 0.51
it has required more expensive and powerful computers.
an eye-catching, if bizarre, moment
were stunningly dysfunctional and weakened by in-
Halloween is DUMB and predictable and DUM
<|endoftext|>rd period, 1

Feature 7

Activation between 4.02 and 4.83
p.m., Pac-12 Network).Some
Activation between 3.22 and 4.02
p.m., Pac-12 Network).Some
12, SEC and Pac-12 — without an
Three schools in the Pac-12 — California,
Activation between 2.41 and 3.22
Activation between 1.61 and 2.41
Cargill, Coca-Cola, General
just six companies: Coca-Cola, General
WWF and The Coca-Cola Company have
6:00 PM PAC-12 NETWORKS
Activation between 0.80 and 1.61
, East, an AFL-CIO affiliated union
the Greater New Orleans AFL-CIO, said
the St. Louis Globe-Democrat said that
union, the Colorado AFL-CIO, is
Activation between 0.00 and 0.80
a source on the Globe-Democrat with information
Bernardo." The Sun-Sentinal promised the
to the University of California at Berkeley to demand my
's plan, CVN-78 will be delivered
<|endoftext|>rd period, 1

Feature 8

Activation between 2.03 and 2.44
duration, and mice of both sexes were protected against
Activation between 1.62 and 2.03
duration, and mice of both sexes were protected against
жидать Brassin и трава
ifax, Nova Scotia, and lived around Nova Scotia
Reviewer: brewster - favorite favorite favorite favorite
such as "Let there be no compulsion in
Activation between 1.22 and 1.62
location of the B. conifer's wings.
Reviewer: redwinter - favorite favorite favorite favorite
ен Совсем ск оро. В
life has its limitations and its drawbacks. So when
oric acid, echinacoside, and ca
Activation between 0.81 and 1.22
'59.99!', 'brand': 'IK
.
ments, Events & more from Tyee and select
be steered from graduation by harsh school
the grounds. That's good—if you
Activation between 0.41 and 0.81
same reason: finding more space at a lower cost
made up of human beings with human
tech giants. For new companies, the ability to
Grade 4 teaching kids how to add five plus four
"Puzzling time to have a review of
Activation between 0.00 and 0.41
one of 10 children from his father's second marriage
a vibrant place for young grads. The average
2. If you find yourself entranced by the
but generated no shortage of interest and media coverage,
<|endoftext|>rd period, 1

Figure 23: Tokens activating the first 9 numerical experts on MxDs with $K = 32$ trained on `Pythia-410m`; we sample 6 bands of activations to show both tokens that highly activate experts and those that activate them only mildly. Magnitude of activation is denoted by the **orange** highlight. Moderate specialism emerges, e.g., to MMO games, abbreviations, and words in specific contexts.

GPT2-124m: Tokens routed to specific experts

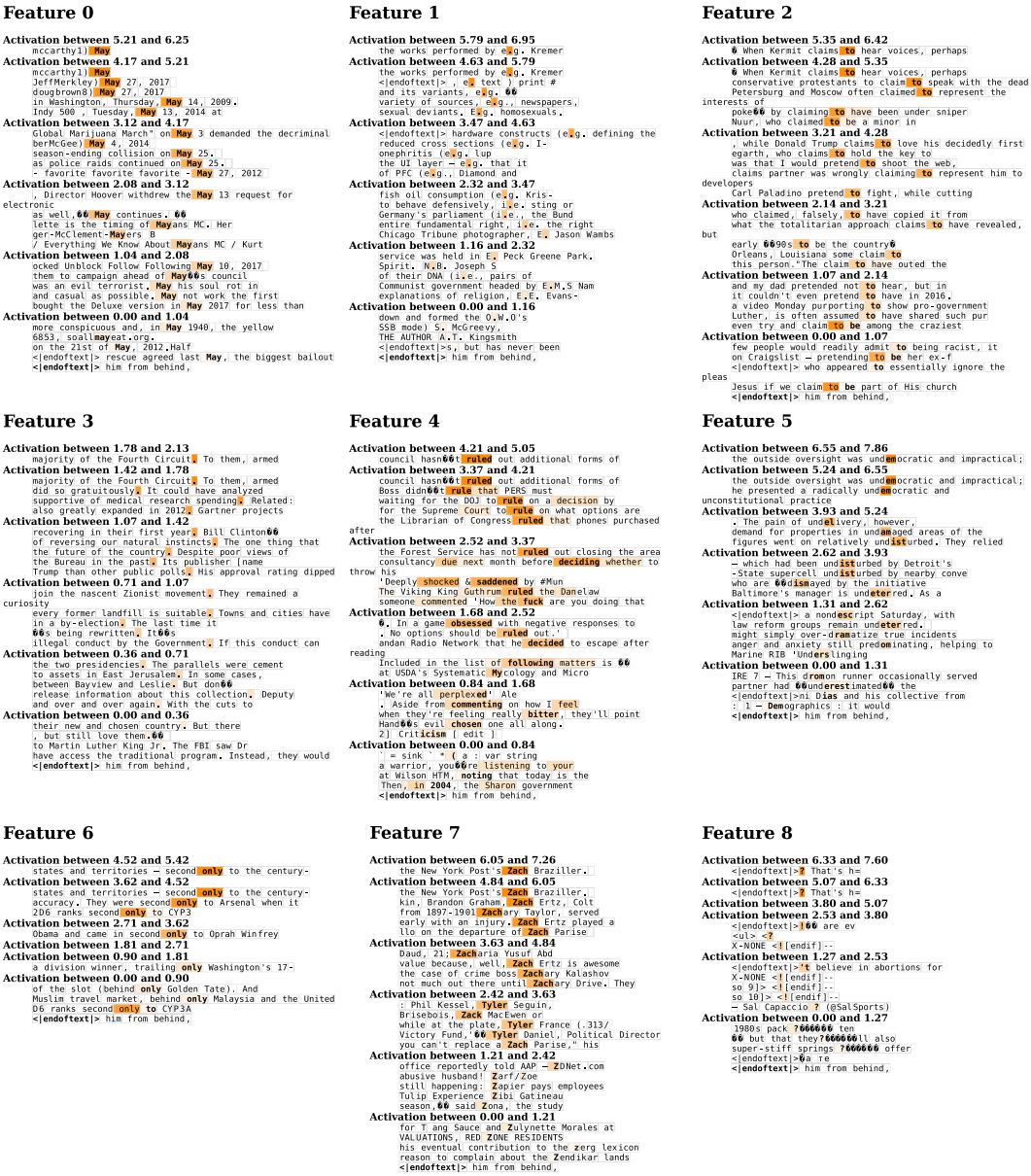

Figure 24: Tokens activating the first 9 numerical experts on MxDs with $K = 32$ trained on `GPT2-124m`; we sample 6 bands of activations to show both tokens that highly activate experts and those that activate them only mildly. Magnitude of activation is denoted by the **orange** highlight. Moderate specialism emerges, e.g., to punctuation, names, and months.